Histopathological examinations of the lungs of mice injected with Ag85B DNA or control DNA and the lungs of healthy naïve mice were performed 25 days after the first inoculation of the plasmid. The lungs of mice that were administered Ag85B DNA on days −7, zero, and 14 did not show any pathological abnormalities compared with those of healthy naïve mice, but the lungs of mice that were administered Ag85B DNA on day 21 showed mild inflammation due to infiltration of eosinophils (Figure 1B). Mice administered the control plasmid did not show any inhibitory effects on the development of allergic inflammations. These results indicated that Ag85B DNA administration was effective for inhibiting the development of allergic inflammation, especially in the early phase of antigen sensitization.

Marked inhibition of allergic immune responses by administration of Ag85B DNA

The levels of protein, total cells, eosinophils, lymphocytes, and neutrophils in BAL fluid from mice immunized with Ag85B DNA vaccine were significantly lower than those in BAL fluid from mice vaccinated with control DNA (Figure 2A–F). Administration of Ag85B DNA also resulted in a significant reduction in the level of OVA-specific IgE (Figure 2G). The concentrations of Th2-type cytokines (IL-5 and IL-13) in BAL fluid from mice immunized with Ag85B DNA vaccine were significantly lower than those in BAL fluid from control mice (Figure 3A and B). These inhibitory effects on the development of allergic inflammation were correlated with day of Ag85B DNA injection. Injection on an early day was more effective for inhibiting the development of allergic inflammation. These results were also confirmed by histopathological observation.

Effects of Ag85B DNA administration on the production of IL-4 and IFN-γ in response to OVA

The production of OVA-specific cytokines in lymph node cells after in vitro stimulation with OVA were assessed. The lymphocytes obtained from thoracic lymph nodes were stimulated in vitro with OVA for 48 hours. IL-4 and IFN-γ levels were measured in culture supernatants by ELISA. The level of IL-4 in culture supernatants from cells of Ag85B DNA-immunized mice was much lower than in culture supernatants from cells of control mice (Figure 4A). On the other hand, the production level of IFN-γ in Ag85B DNA-immunized mice was significantly higher than in control DNA-immunized mice (Figure 4B).

Expression of cytokine mRNA in pulmonary lymph node cells after stimulation with OVA

The production of OVA-specific cytokines was also confirmed by mRNA levels of Th1-type cytokines (IFN-γ, IL-2, and IL-12) and Th2-type cytokines (IL-4, IL-5, and IL-13) (Figure 5A–C). Lymph node cells from Ag85B DNA vaccine-immunized mice showed strong IFN-γ, IL-2, and IL-12 expression and weak IL-4, IL-5, and IL-13 expression of mRNA, whereas control DNA-immunized mice showed the completely opposite results. The cells from control mice showed strong mRNA expression of Th2-type cytokines and weak mRNA expression of Th1-type cytokines (Figure 5A–C). It has been reported that therapeutic effects against asthma by administration of the culture supernatant of *M. vaccae* were derived from Treg cells by the induction of IL-10 and transforming growth factor-β.[16] In the current study, mRNA expression levels of IL-10 and transforming growth factor-β in lymph node cells obtained from mice immunized with Ag85B DNA were much higher than those in lymph node cells obtained from control mice after in vitro stimulation with OVA (Figure 5A and D). Another Th17 cell lineage, which is associated with allergen-induced airway allergic inflammation, was also assessed by the mRNA expression of cytokines. In the current experiment, mRNA expression of IL-17 was seen in both control DNA-immunized and Ag85B-DNA immunized mice after stimulation with OVA, with no difference in the mRNA expression levels of IL-17 between these groups (Figure 5A and E). The mRNA expression of IL-23 was also assessed since IL-23 is associated with the maturation of Th17 cells.[17] Expression of IL-23 mRNA was observed at the same level in all samples (Figure 5A and E). Inhibitory effects on the development of allergic inflammation are readily obtained in a mouse model of asthma through the administration of Ag85B DNA. These effects of immunotherapy by Ag85B DNA are due to activation of the immune responses of Th1 and Treg cells and inhibition of the responses of Th2 cells as a result of the enhancement of responses of Th1 and Treg cells.

Discussion

Current treatments of nonspecific immunosuppressive therapy for asthma, such as administration of glucocorticoids, are not satisfactory. Although these treatments are highly effective for controlling disease, most patients must continue to take these drugs throughout their lives. Moreover, these drugs have side effects, and asthma cannot be controlled by these drugs in up to 30% of patients. Given the high prevalence

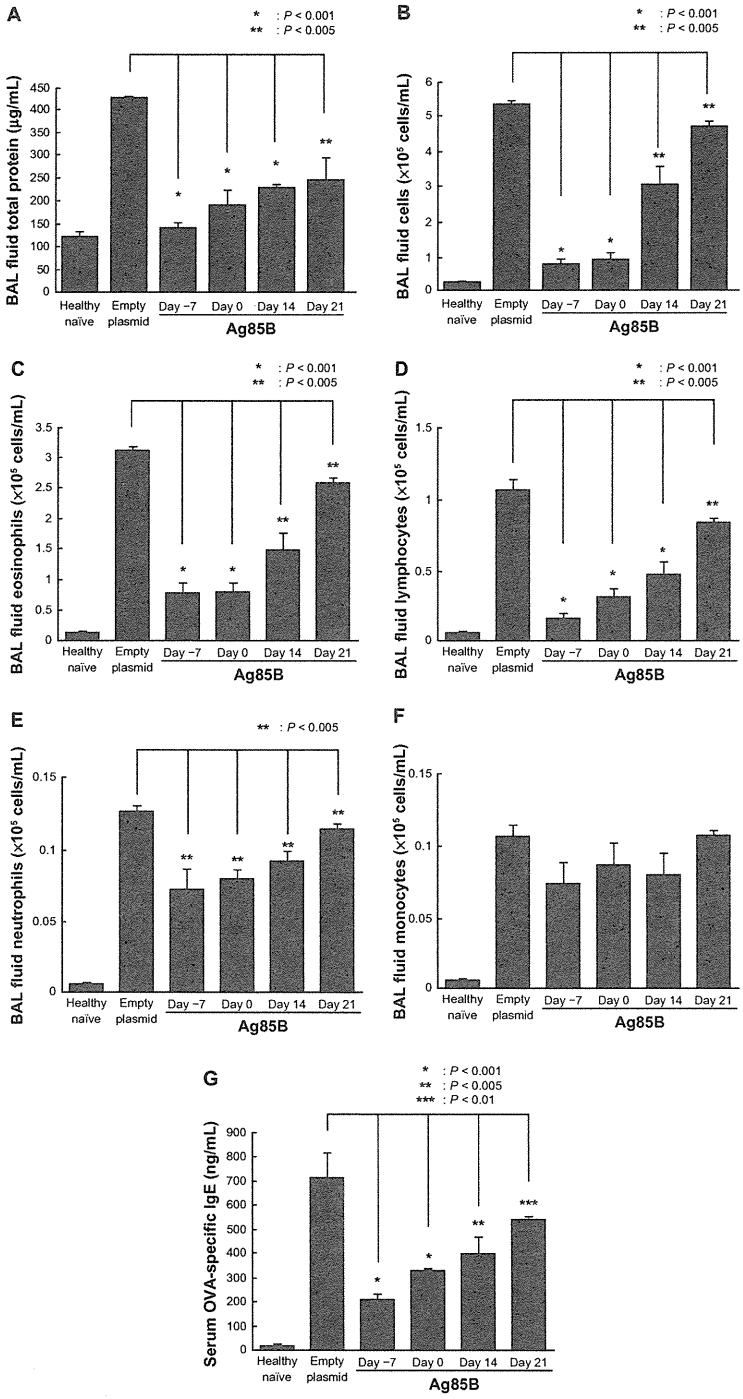

Figure 2 Marked inhibition of the development of allergic inflammation by administration of Ag85B DNA. BAL fluid was obtained by injecting and recovering two 0.5 mL aliquots of phosphate-buffered saline via a tracheal cannula. Cells in the lavage fluid were counted using a hematocytometer, and the differentials were determined by utilizing light microscopy to count 300 cells on Cytospin® preparations (Thermo Fisher Scientific, Waltham, MA). The concentration of inflammatory protein was measured by Protein Assay Reagent (Bio-Rad Laboratories, Hercules, CA). Results for healthy naïve mice and control plasmid DNA-immunized mice are also shown. (**A**) Total protein, (**B**) number of cells, (**C**) eosinophils, (**D**) lymphocytes, (**E**) neutrophils, and (**F**) monocytes in BAL fluid from experimental animals were investigated. (**G**) The degrees of ovalbumin-specific immunoglobulin E responses in sera collected from experimental mice were also analyzed. Immunoglobulin E levels in sera were measured using enzyme-linked immunosorbent assay kits according to the procedure recommended by the manufacturer (Shibayagi Co, Ltd, Shibukawa, Japan). BAL fluid and sera were collected 25 days after the first ovalbumin immunization.

Notes: Data are representative of at least three independent experiments; values shown are the means and standard deviations of five mice per group; statistical analysis was performed using the Mann–Whitney U test and the Kruskal–Wallis test.

Abbreviations: Ag85B, antigen 85B; BAL, bronchoalveolar lavage.

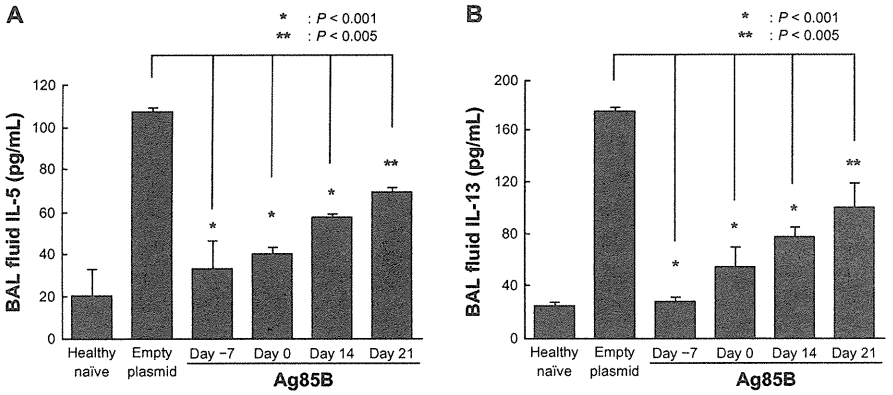

Figure 3 IL-5 and IL-13 production in BAL fluid. Amounts of (**A**) IL-5 and (**B**) IL-13 in BAL fluid were measured using an enzyme-linked immunosorbent assay kit (R&D Systems, Minneapolis, MN) 25 days after the first ovalbumin immunization.
Notes: Data are representative of at least three independent experiments; values shown are means and standard deviations of five mice per group; statistical analysis was performed using the Mann–Whitney U test and the Kruskal–Wallis test.
Abbreviations: Ag85B, antigen 85B; BAL, bronchoalveolar lavage; IL, interleukin.

of this disease, improved and more effective therapeutic strategies are needed. The results of many studies have suggested that effective immunotherapy for allergic disease is associated with immune deviation from a disease-promoting Th2 response towards a Th1 response, with Treg cells having appropriate functions (reviewed in Takeda et al).[18] In the current study, the applicability of plasmid encoding complementary DNA of Ag85B from mycobacteria DNA to gene therapy of asthma was assessed. Although the introduced DNA is expressed predominantly by somatic cells, it is known that a relatively small but biologically significant number of dendritic cells are transfected with the inoculated DNA.[19–21] Moreover, it was recently reported that systemic inoculation of a plasmid DNA may cause dendritic cell activation through direct transfection into dendritic cells.[22] It was demonstrated that inhibitory effects on the development of allergic inflammation are readily obtained in a mouse model of asthma through the administration of Ag85B DNA, even with only a single administration before or after antigen sensitization.

The mechanism of immune responses induced by Ag85B remains unclear. Various products having adjuvant activities, eg, lipopolysaccharide, cytosine-phosphodiester-guanine motif, and polyinosinic:polycytidylic acid, involve toll-like receptors (TLRs) and show augmentation of Th1-type immune responses.[18] It was previously reported that plasmid DNA encoding Ag85B stimulated the expression of TLR2, TLR3, and TLR4 mRNA. One possibility is that the induction

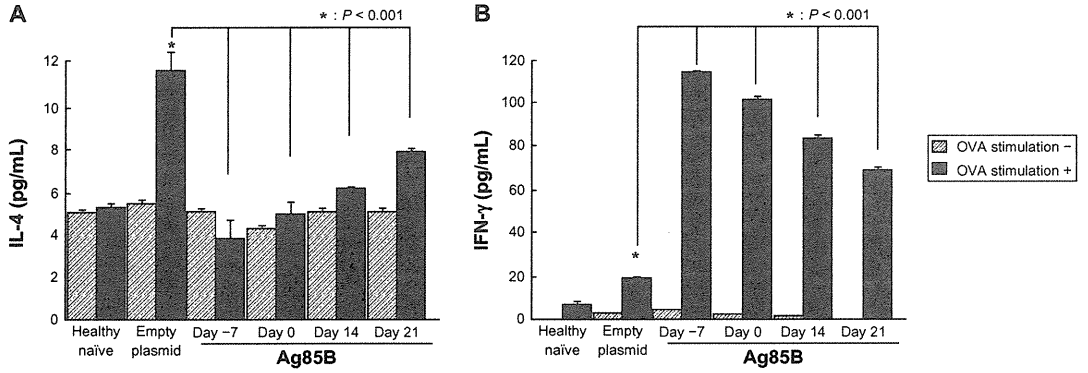

Figure 4 IFN-γ and IL-4 production in culture supernatant. Amounts of (**A**) IFN-γ and (**B**) IL-4 in culture supernatant were measured by enzyme-linked immunosorbent assay 25 days after the first OVA immunization. Spleen cells from immunized mice (5×10^6) were cultured with 10 μg/mL OVA in 24-well culture plates at a volume of 2 mL. After incubation at 37°C in a humidified incubator (5% carbon dioxide) for 96 hours, culture supernatants were quantified by using a standard enzyme-linked immunosorbent assay kit (Life Technologies, Carlsbad, CA).
Notes: Data are representative of at least three independent experiments; values represent mean and standard deviation of ten mice per group; statistical analysis was performed using the Mann–Whitney U test and the Kruskal–Wallis test.
Abbreviations: Ag85B, antigen 85B; IFN-γ, interferon-γ; IL-4, interleukin-4; OVA, ovalbumin.

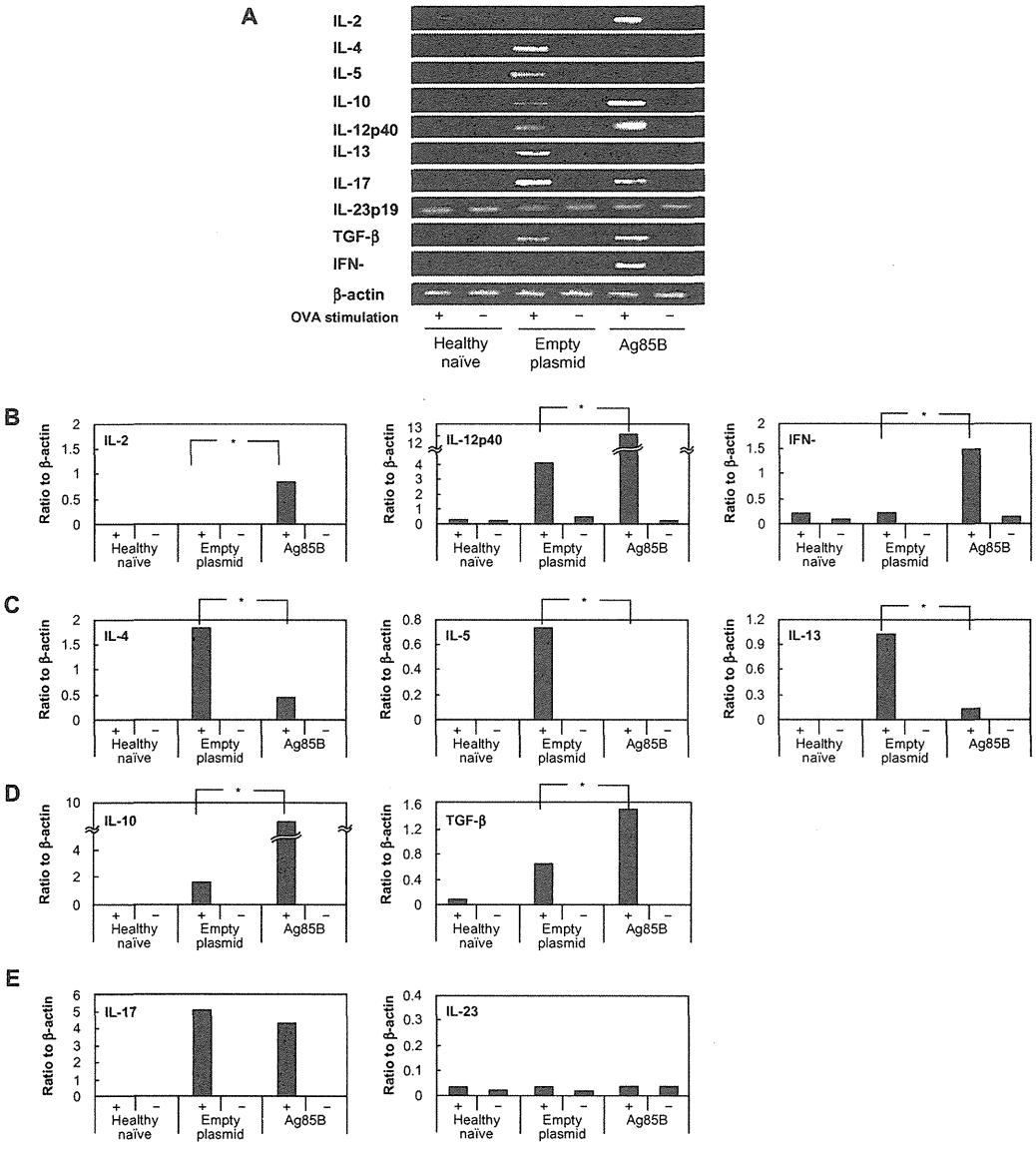

Figure 5 Detection of cytokine messenger ribonucleic acid from lymphocytes using real-time polymerase chain reaction. Spleen cells were stimulated in vitro with OVA for 1 day in culture. Spleen cells stimulated with fetal calf serum were used as controls. Total ribonucleic acid was purified from the OVA-stimulated or fetal calf serum (control)-stimulated spleen cells using Isogen (Nippon Gene Co, Ltd, Tokyo, Japan) following the manufacturer's instructions. For the real-time reaction, a reverse transcription system (Promega Corporation, Fitchburg, WI) was used. Polymerase chain reaction was performed in a total volume of 50 μL of 1 × polymerase chain reaction buffer (Takara Shuzo, Kyoto, Japan) containing 0.5–1.0 μg of complementary DNA, 0.25 mM of each deoxyribonucleotide triphosphate, 2 μM of each primer, and 2.5 U of *Taq* DNA polymerase (Takara Shuzo). The specific primer pairs used were previously described.[15] The samples were amplified for 30–35 cycles under the following conditions: annealing for 30 seconds at 56°C, extension for 1 minute at 73°C, and denaturation for 30 seconds at 93°C. (**A**) The reaction products were analyzed on 2% agarose, Tris-buffered ethylenediaminetetraacetic acid gels. (**B–E**) Photographs of the gels were scanned, and band intensities were measured using a densitometer (CS Analyzer 3.0; ATTO Corporation, Tokyo, Japan). The quantity of cytokine messenger ribonucleic acid was determined by the ratio of cytokine and beta actin band intensities.

Notes: *$P < 0.005$; the profiles are representative of three independent experiments; statistical analysis was performed using the Mann–Whitney U test and the Kruskal–Wallis test.

Abbreviations: Ag85B, antigen 85B; IFN-γ, interferon-γ; IL, interleukin; OVA, ovalbumin; TGF-β, transforming growth factor-β.

of Th1-type immune responses by Ag85B is involved in innate immune responses. From this result, the activation of Th1 and Treg cells by Ag85B administration was thought to be involved in responses through stimulation of TLR2, TLR3, and TLR4, but not TLR9.[14] Various proteins derived from pathogens promote Th1 responses through stimulation of TLRs and subsequently through secretion of cytokines.[18] It has also been reported that TLR signaling induces not only Th1-type immune responses but also secretion of various cytokines from Treg cells.[23–27] Moreover, recent studies have

indicated that Th1 cells produce IL-10 as well as Th1-type cytokines by Notch regulation-dependent signal transducer and activator of transcription-4 signaling.[28] From these findings, effective immunotherapy by induction of both Th1 cell and Treg cell responses is thought to be possible by using appropriate materials. In fact, an asthma model of mice immunized with culture supernatant of mycobacteria, *M. vaccae*, showed Th1 and Treg responses.[16] The results of the current study suggest that the administration of Ag85B DNA has several potential advantages due to the activation of Th1 and Treg cells for the prevention and treatment of asthma.

Immunization with mycobacteria or mycobacteria products has been reported to inhibit the development of allergic disease.[29–32] However, various causative factors affect immune responses by mycobacteria. It was reported as a notable point that the efficacy of mycobacteria in preventing allergic inflammation of asthma was strongly affected by *Nramp1* alleles.[33] Several host genetic factors, including natural resistance-associated macrophage protein 1 (NRAMP1),[34] vitamin D receptor (VDR),[35,36] and Mendelian susceptibility to mycobacterial disease,[37] have been reported to be involved in responses to mycobacteria (reviewed in Casanova and Abel).[38] Differences in immune responses induced by different mycobacteria strains have also been reported. The differential immune responses were mediated by lipid-extracted molecules of mycobacteria.[39] Moreover, environmental factors are important for immune responses induced by mycobacteria in therapy for atopic diseases.[40,41] Presensitization of mycobacteria in the natural environment affects the induction of Th1-type immune responses by mycobacteria vaccination.[9,42,43] However, the specific components of mycobacteria that inhibit the development of allergic responses have not been reported. Ag85B is a single component of mycobacteria, and this product might not be affected by various other mycobacteria factors involved in immune responses. In fact, Th1-type immune responses induced by Ag85B are not affected by *Nramp* in mice.[44,45]

Wu et al demonstrated the effects of intranasal administration of Ag85B in a mouse model of asthma.[46] It was previously reported that Ag85B has strong adjuvant activities involving Th1 immune responses.[14] Intranasal administration of a plasmid DNA (DNA vaccine) with adjuvant activities has been considered to be inappropriate for human use. Intranasal inactivated influenza vaccine, with adjuvant, induced Bell's palsy in humans. Therefore, intranasal inactivated influenza vaccine with adjuvant is no longer in clinical use.[47] Systemic administration of a plasmid DNA (DNA vaccine) is better than intranasal administration if the same effects of the plasmid DNA can be induced. The current study demonstrated the usefulness of Ag85B DNA vaccine and provided evidence of the potential utility of Ag85B DNA vaccine for the prevention and treatment of asthma, even with only a single systemic administration before or after antigen sensitization.

Conclusion

The correction of immune response should be considered in the prevention and treatment of asthma. Ag85B has potential utility for the prevention and treatment of asthma even with only a single administration.

Acknowledgments

This work was supported by Health Science Research Grants from the Ministry of Health, Labor, and Welfare of Japan and the Ministry of Education, Culture, Sports, Science, and Technology of Japan.

Disclosure

The authors report no conflicts of interest in this work.

References

1. Umetsu DT, DeKruyff RH. TH1 and TH2 CD4+ cells in human allergic diseases. *J Allergy Clin Immunol*. 1997;100(1):1–6.
2. Wills-Karp M, Luyimbazi J, Xu X, et al. Interleukin-13: central mediator of allergic asthma. *Science*. 1998;282(5397):2258–2261.
3. Lambrecht BN, Hammad H. The airway epithelium in asthma. *Nat Med*. 2012;18(5):684–692.
4. Bentley AM, Meng Q, Robinson DS, Hamid Q, Kay AB, Durham SR. Increases in activated T lymphocytes, eosinophils, and cytokine mRNA expression for interleukin-5 and granulocyte/macrophage colony-stimulating factor in bronchial biopsies after allergen inhalation challenge in atopic asthmatics. *Am J Respir Cell Mol Biol*. 1993;8(1):35–42.
5. Bossley CJ, Fleming L, Gupta A, et al. Pediatric severe asthma is characterized by eosinophilia and remodeling without T(H)2 cytokines. *J Allergy Clin Immunol*. 2012;129(4):974–982.e13.
6. Akdis CA, Akdis M. Mechanisms and treatment of allergic disease in the big picture of regulatory T cells. *J Allergy Clin Immunol*. 2009;123(4):735–746.
7. Hawrylowicz CM, O'Garra A. Potential role of interleukin-10-secreting regulatory T cells in allergy and asthma. *Nat Rev Immunol*. 2005;5(4):271–283.
8. Racila DM, Kline JN. Perspectives in asthma: molecular use of microbial products in asthma prevention and treatment. *J Allergy Clin Immunol*. 2005;116(6):1202–1205.
9. Krishna MT, Salvi SS. Could administration of bacille Calmette-Guerin vaccination at birth protect from the development of asthma and allergic diseases in the western world? Has this question been adequately investigated? *Pediatr Allergy Immunol*. 2002;13(3):172–176.
10. Harada M, Magara-Koyanagi K, Watarai H, et al. IL-21-induced Bepsilon cell apoptosis mediated by natural killer T cells suppresses IgE responses. *J Exp Med*. 2006;203(13):2929–2937.
11. Arnoldussen DL, Linehan M, Sheikh A. BCG vaccination and allergy: a systematic review and meta-analysis. *J Allergy Clin Immunol*. 2011;127(1):246–253.
12. Tamura T, Ariga H, Kinashi T, et al. The role of antigenic peptide in CD4+ T helper phenotype development in a T cell receptor transgenic model. *Int Immunol*. 2004;16(12):1691–1699.

13. Kuromatsu I, Matsuo K, Takamura S, et al. Induction of effective antitumor immune responses in a mouse bladder tumor model by using DNA of an alpha antigen from mycobacteria. *Cancer Gene Ther.* 2001;8(7):483–490.
14. Takamura S, Matsuo K, Takebe Y, Yasutomi Y. Ag85B of mycobacteria elicits effective CTL responses through activation of robust Th1 immunity as a novel adjuvant in DNA vaccine. *J Immunol.* 2005;175(4):2541–2547.
15. Nishikubo K, Murata Y, Tamaki S, et al. A single administration of interleukin-4 antagonistic mutant DNA inhibits allergic airway inflammation in a mouse model of asthma. *Gene Ther.* 2003;10(26):2119–2125.
16. Zuany-Amorim C, Sawicka E, Manlius C, et al. Suppression of airway eosinophilia by killed Mycobacterium vaccae-induced allergen-specific regulatory T-cells. *Nat Med.* 2002;8(6):625–629.
17. Korn T, Bettelli E, Oukka M, Kuchroo VK. IL-17 and Th17 cells. *Annu Rev Immunol.* 2009;27:485–517.
18. Takeda K, Kaisho T, Akira S. Toll-like receptors. *Annu Rev Immunol.* 2003;21:335–376.
19. Tuting T, Storkus WJ, Falo LD Jr. DNA immunization targeting the skin: molecular control of adaptive immunity. *J Invest Dermatol.* 1998;111(2):183–188.
20. Condon C, Watkins SC, Celluzzi CM, Thompson K, Falo LD Jr. DNA-based immunization by in vivo transfection of dendritic cells. *Nat Med.* 1996;2(10):1122–1128.
21. Porgador A, Irvine KR, Iwasaki A, Barber BH, Restifo NP, Germain RN. Predominant role for directly transfected dendritic cells in antigen presentation to CD8+ T cells after gene gun immunization. *J Exp Med.* 1998;188(6):1075–1082.
22. Tajiri K, Imanaka-Yoshida K, Matsubara A, et al. Suppressor of cytokine signaling 1 DNA administration inhibits inflammatory and pathogenic responses in autoimmune myocarditis. *J Immunol.* 2012;189(4):2043–2053.
23. Lloyd CM, Hawrylowicz CM. Regulatory T cells in asthma. *Immunity.* 2009;31(3):438–449.
24. Jin B, Shun T, Yu XH, Yang YX, Yeo AE. The effects of TLR activation on T-cell development and differentiation. *Clin Dev Immunol.* 2012;2012:836485.
25. Ouabed A, Hubert FX, Chabannes D, Gautreau L, Heslan M, Josien R. Differential control of T regulatory cell proliferation and suppressive activity by mature plasmacytoid versus conventional spleen dendritic cells. *J Immunol.* 2008;180(9):5862–5870.
26. Jarnicki AG, Conroy H, Brereton C, et al. Attenuating regulatory T cell induction by TLR agonists through inhibition of p38 MAPK signaling in dendritic cells enhances their efficacy as vaccine adjuvants and cancer immunotherapeutics. *J Immunol.* 2008;180(6):3797–3806.
27. Bell MP, Svingen PA, Rahman MK, Xiong Y, Faubion WA Jr. FOXP3 regulates TLR10 expression in human T regulatory cells. *J Immunol.* 2007;179(3):1893–1900.
28. Rutz S, Janke M, Kassner N, Hohnstein T, Krueger M, Scheffold A. Notch regulates IL-10 production by T helper 1 cells. *Proc Natl Acad Sci U S A.* 2008;105(9):3497–3502.
29. Herz U, Gerhold K, Gruber C, et al. BCG infection suppresses allergic sensitization and development of increased airway reactivity in an animal model. *J Allergy Clin Immunol.* 1998;102(5):867–874.
30. Wang CC, Rook GA. Inhibition of an established allergic response to ovalbumin in BALB/c mice by killed Mycobacterium vaccae. *Immunology.* 1998;93(3):307–313.
31. Yang X, Wang S, Fan Y, Zhu L. Systemic mycobacterial infection inhibits antigen-specific immunoglobulin E production, bronchial mucus production and eosinophilic inflammation induced by allergen. *Immunology.* 1999;98(3):329–337.
32. Cavallo GP, Elia M, Giordano D, Baldi C, Cammarota R. Decrease of specific and total IgE levels in allergic patients after BCG vaccination: preliminary report. *Arch Otolaryngol Head Neck Surg.* 2002;128(9):1058–1060.
33. Bellamy R. Susceptibility to mycobacterial infections: the importance of host genetics. *Genes Immun.* 2003;4(1):4–11.
34. Smit JJ, Van Loveren H, Hoekstra MO, Karimi K, Folkerts G, Nijkamp FP. The Slc11a1 (Nramp1) gene controls efficacy of mycobacterial treatment of allergic asthma. *J Immunol.* 2003;171(2):754–760.
35. Bellamy R, Ruwende C, Corrah T, et al. Tuberculosis and chronic hepatitis B virus infection in Africans and variation in the vitamin D receptor gene. *J Infect Dis.* 1999;179(3):721–724.
36. Yang HF, Zhang ZH, Chang ZQ, Tang KL, Lin DZ, Xu JZ. Vitamin D deficiency affects the immunity against Mycobacterium tuberculosis infection in mice. *Clin Exp Med.* August 10, 2012. [Epub ahead of print.]
37. Reichenbach J, Rosenzweig S, Doffinger R, Dupuis S, Holland SM, Casanova JL. Mycobacterial diseases in primary immunodeficiencies. *Curr Opin Allergy Clin Immunol.* 2001;1(6):503–511.
38. Casanova JL, Abel L. Genetic dissection of immunity to mycobacteria: the human model. *Annu Rev Immunol.* 2002;20:581–620.
39. Manca C, Reed MB, Freeman S, et al. Differential monocyte activation underlies strain-specific Mycobacterium tuberculosis pathogenesis. *Infect Immun.* 2004;72(9):5511–5514.
40. Arkwright PD, David TJ. Effect of Mycobacterium vaccae on atopic dermatitis in children of different ages. *Br J Dermatol.* 2003;149(5):1029–1034.
41. Arkwright PD, David TJ. Intradermal administration of a killed Mycobacterium vaccae suspension (SRL 172) is associated with improvement in atopic dermatitis in children with moderate-to-severe disease. *J Allergy Clin Immunol.* 2001;107(3):531–534.
42. Martignon G, Oryszczyn MP, Annesi-Maesano I. Does childhood immunization against infectious diseases protect from the development of atopic disease? *Pediatr Allergy Immunol.* 2005;16(3):193–200.
43. Choi IS, Koh YI. Effects of BCG revaccination on asthma. *Allergy.* 2003;58(11):1114–1116.
44. Lozes E, Huygen K, Content J, et al. Immunogenicity and efficacy of a tuberculosis DNA vaccine encoding the components of the secreted antigen 85 complex. *Vaccine.* 1997;15(8):830–833.
45. Baldwin SL, D'Souza CD, Orme IM, et al. Immunogenicity and protective efficacy of DNA vaccines encoding secreted and non-secreted forms of Mycobacterium tuberculosis Ag85A. *Tuber Lung Dis.* 1999;79(4):251–259.
46. Wu J, Xu J, Cai C, Gao X, Li L, Zhong N. Ag85B DNA vaccine suppresses airway inflammation in a murine model of asthma. *Respir Res.* 2009;10:51.
47. Mutsch M, Zhou W, Rhodes P, et al. Use of the inactivated intranasal influenza vaccine and the risk of Bell's palsy in Switzerland. *N Engl J Med.* 2004;350(9):896–903.

Arch Virol
DOI 10.1007/s00705-011-1178-6

BRIEF REPORT

$CD16^+$ natural killer cells play a limited role against primary dengue virus infection in tamarins

Tomoyuki Yoshida · Tsutomu Omatsu · Akatsuki Saito · Yuko Katakai · Yuki Iwasaki · Sayuki Iijima · Terue Kurosawa · Masataka Hamano · Shinichiro Nakamura · Tomohiko Takasaki · Yasuhiro Yasutomi · Ichiro Kurane · Hirofumi Akari

Received: 29 July 2011 / Accepted: 12 November 2011

Abstract CD16 is a major molecule expressed on NK cells. To directly assess the role of natural killer (NK) cells in dengue virus (DENV) infection *in vivo*, CD16 antibody-treated tamarins were inoculated with a DENV-2 strain. This resulted in the transient depletion of $CD16^+$ NK cells, whereas no significant effects on the overall levels or kinetics of plasma viral loads and antiviral antibodies were observed in the treated monkeys when compared to control monkeys. It remains elusive whether the $CD16^-$ NK subpopulation could play an important role in the control of primary DENV infection.

Keywords Dengue virus · Tamarin · NK cells · CD16

T. Yoshida and T. Omatsu contributed equally to this study.

Electronic supplementary material The online version of this article (doi:10.1007/s00705-011-1178-6) contains supplementary material, which is available to authorized users.

T. Yoshida · Y. Iwasaki · S. Iijima · T. Kurosawa · M. Hamano · Y. Yasutomi · H. Akari
Tsukuba Primate Research Center, National Institute of Biomedical Innovation, 1-1 Hachimandai, Tsukuba, Ibaraki 305-0843, Japan

T. Yoshida (✉) · A. Saito · H. Akari (✉)
Center for Human Evolution Modeling Research, Primate Research Institute, Kyoto University, Inuyama, Aichi 484-8506, Japan
e-mail: ytomoyuki@pri.kyoto-u.ac.jp

H. Akari
e-mail: akari@pri.kyoto-u.ac.jp

T. Omatsu · T. Takasaki · I. Kurane
Department of Virology I, National Institute of Infectious diseases, 1-23-1 Toyama, Shinjuku-ku, Tokyo 162-8640, Japan

DENV is one of the most serious mosquito-borne virus affecting humans, with 2.5 billion people at risk in tropical and subtropical regions around the world each year [12]. A wide variety of clinical manifestations have been noted, which range from asymptomatic, mild febrile illness (dengue fever [DF]) to dengue hemorrhagic fever (DHF)/dengue shock syndrome (DSS), a life-threatening illness. It has been shown that humans with a secondary heterologous DENV infection are at a higher risk of contracting severe dengue disease [10, 26]. DHF/DSS occurs in infants during primary DENV infection, predominantly in the second half of the first year of life, when maternal antibodies have low residual neutralizing activity [11, 17].

NK cells are a component of the innate immune system that plays a central role in host defense against viral infection and tumor cells. It has been shown that infection by some viruses, such as herpes simplex virus-1, influenza virus or ectromelia poxvirus, can be controlled by NK cells in mice [15]. Yet the most compelling evidence for a role

A. Saito
International Research Center for Infectious Diseases, The Institute of Medical Science, The University of Tokyo, 4-6-1 Shirokanedai, Minato-ku, Tokyo 108-8639, Japan

Y. Katakai
Corporation for Production and Research of Laboratory Primates, 1-1 Hachimandai, Tsukuba, Ibaraki 305-0843, Japan

S. Nakamura
Research Center for Animal Life Science, Shiga University of Medical Science, Seta Tsukinowa-cho, Otsu, Shiga 520-2192, Japan

Published online: 03 December 2011

of NK cells in early defense against viruses was obtained in a study showing increased susceptibility to murine cytomegalovirus (MCMV) after NK cell depletion and increased resistance after adoptive transfer of NK cells [23]. Defects in NK cell activity, such as decreased production of interferon (IFN)-γ or cytotoxicity, render mice more susceptible to MCMV infection [23]. NK cells can kill virus-infected cells by using cytotoxic granules or by recognizing and inducing lysis of antibody-coated target cells (antibody-dependent cell cytotoxicity) via an Fc-binding receptor such as CD16 [21].

Early activity of NK cells may be important for clearing primary DENV infection [24]. In a DENV mouse model, mice experimentally infected with DENV showed increased NK cell levels [24]. A significant increase in the frequency of NK cell circulation was also shown in patients who developed an acute dengue disease [2]. In addition, patients with a mild dengue disease have elevated NK cell rates when compared to those with severe dengue diseases [9, 27]. Moreover, Kurane *et al.* [14] reported that human blood NK cells are cytotoxic against DENV-infected cells in target organs via direct cytolysis and antibody-dependent cell-mediated cytotoxicity. It was also shown that the intracellular cytotoxic granule, TIA-1, was up-regulated early in NK cells in the acute phase of DENV infection and that NK-activating receptor NKp44 was involved in virus-mediated NK activation through direct interaction with DENV envelope protein [2, 13]. These results suggest that the early activation of NK cells contributes to the prevention of the severe dengue disease. However, based on quantitative and functional analyses in animal models *in vivo*, defining the contribution of NK cells to suppression of DENV replication *in vivo* has been necessary.

We have recently reported that common marmosets (*Callithrix jacchus*) are highly permissive to DENV infection [22]. These New World monkeys, being nonhuman primates, are considered to have an immune system similar to that of humans [28, 29]. The present study was initiated to investigate the role of NK cells in controlling DENV during primary infection in our nonhuman primate model.

The animals were cared for in accordance with National Institute of Biomedical Innovation rules and guidelines for experimental animal welfare, and all protocols were approved by our Institutional Animal Study Committee. Eight tamarins (*Saguinus midas* and *Saguinus labiatus*) were used in this study. As marmosets and tamarins are closely related monkey species and are classified as members of the Callitrichinae, we expected that tamarins would also be permissive to DENV infection, like marmosets. To check the permissiveness of tamarins to DENV, 2 tamarins were infected with DENV-2 (DHF0663 strain: 6.7×10^7 PFU/ml) subcutaneously or intravenously (Fig. 1).

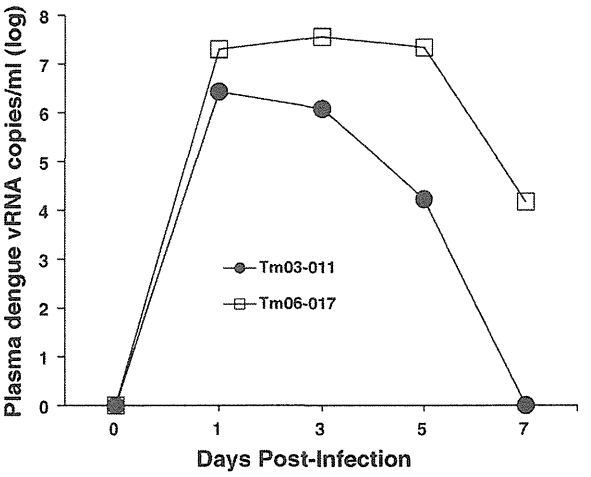

Fig. 1 Levels of vRNA in DENV-infected tamarins. Tamarins were infected subcutaneously or intravenously with DENV at a dose of 6.7×10^7 PFU/ml. The vRNAs were detected in plasma by real-time PCR. Tm03-011, subcutaneous infection; Tm06-017, intravenous infection

Dengue viral RNA (vRNA), which was quantified using real-time PCR as previously described [22], was detected in plasma samples from the tamarins on day 1 post-infection. For each of the two tamarins (Tm03-011, Tm06-017), the plasma vRNA levels reached 2.7×10^6 copies/ml and 2.0×10^7 copies/ml on day 1 post-infection, respectively, and were detectable on days 3 and 5. These results indicate that tamarins are also permissive to DENV infection, which is consistent with the results obtained by using marmosets [22].

Next, we sought to assess the role of NK cells in DENV infection *in vivo*. In this regard, in vivo depletion of NK cells by the administration of NK-specific monoclonal antibody (mAb) was considered to be straightforward to directly address the question. We employed a new method by which an anti-CD16 mAb 3G8 [7] but not a control mAb MOPC-21 efficiently depleted a major NK population expressing CD16 in tamarins, as we recently reported [29]. The mouse anti-human CD16 mAb 3G8 was produced in serum-free medium and purified using protein A affinity chromatography. Endotoxin levels were confirmed to be lower than 1 EU/mg. Four red-handed tamarins and two white-lipped tamarins (*Saguinus labiatus*) were used in this experiment. Three tamarins were intravenously administered 3G8 at a dose of 50 mg/kg, while others were given a control mAb MOPC-21. One day later, both mAb-treated tamarins were subcutaneously inoculated with 3×10^5 PFU/ml of DENV-2 DHF0663 strain on the basis of a previous report that a single mosquito might inject between 10^4 and 10^5 PFU of DENV into a human [20]. It was confirmed that at 1-3 days after the 3G8 mAb treatment, $CD16^+$ cells were almost completely depleted in the

tamarins followed by recovery to the initial levels at around 2 weeks after administration, while the cells were maintained at the initial levels in the monkeys with MOPC-21 (Fig. 2a). In addition, it is noteworthy that the ratios of $CD4^+$ and $CD8^+$ T cells and $CD20^+$ B cells were not affected by the administration of the 3G8 mAb (Supplementary Figure 1). In the case of administration of mAb MOPC-21, we confirmed no significant effect on $CD16^+$ cells (Supplementary Figure 2). The killing activities of the peripheral blood mononuclear cells (PBMCs) taken from the 3G8-treated monkeys were reduced at day 1 post-antibody-treatment, followed by an increase irrespective of depletion of $CD16^+$ NK cells at day 2 post-antibody-treatment (1 day after DENV inoculation), suggesting that the $CD16^-$ NK population may be activated by DENV infection (Fig. 2b). Plasma viral loads in both mAb-treated monkeys rose to 10^5 copies/ml by day 1 after infection and then reached a peak at 10^6 copies/ml on day 3 or day 7, followed by a rapid decline, with values dipping below the detectable level by day 14 after infection (Fig. 2c). These results suggested that $CD16^+$ NK cells apparently did not contribute to DENV replication in the acute phase in our tamarin model.

It was reported previously that non-structural glycoprotein NS1 is essential for flavivirus viability and that the NS1 protein circulates during the acute phase of disease in the plasma of patients infected with DENV [1]. Epidemiological studies have demonstrated that secreted NS1 levels are correlated with viremia levels and are higher in cases of DHF than in dengue fever (DF) early in illness [16]. Thus, it has been suggested that NS1 might be a useful marker as an indicator of the severity of dengue disease. We have used the level of the NS1 antigen as an alternative diagnostic marker to examine the effects of CD16 antibody treatment on DENV replication. The NS1 was measured by Platelia Dengue NS1 Ag assay (BioRad). Antigenemia was observed in these infected monkeys between 3-14 days post-infection. Serum IgM and IgG specific for DENV antigens were measured by ELISA. DENV-specific IgM or IgG antibody was equally detected in both mAb-treated monkeys (Fig. 3).

We recently demonstrated that marmosets are permissive to DENV infection [22]. In this study, we found that tamarins are also permissive to DENV infection (Fig. 1). Moreover, we also investigated the role of NK cells against early DENV infection using *in vivo* depletion of $CD16^+$

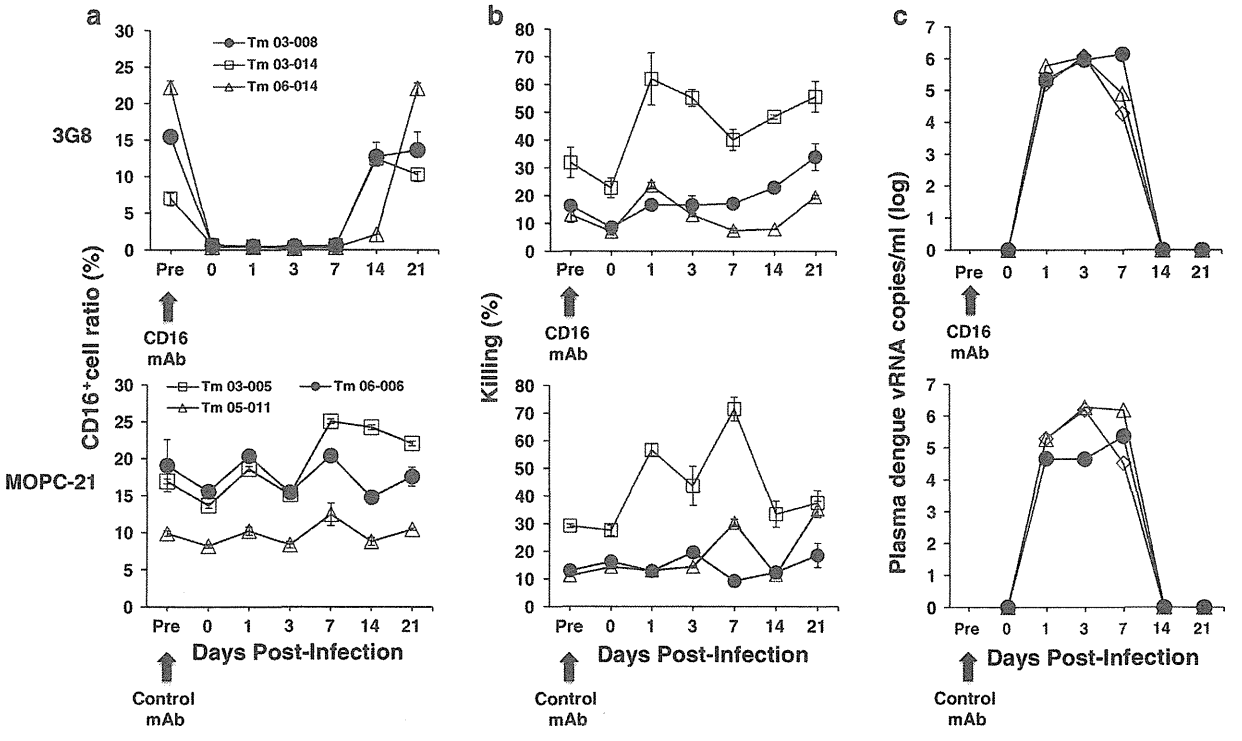

Fig. 2 Ratios of $CD16^+$ NK cells, killing activity of PBMCs, and vRNA in DENV-infected tamarins after treatment with 3G8 or MOPC-21 mAb. Tamarins were infected subcutaneously with DENV at a dose $3x10^5$ PFU/ml after treatment with 50 mg/kg of 3G8 or MOPC-21 mAb. **a** Ratios of $CD16^+$ NK cells were determined in whole-blood specimens. **b** The activities of NK cells were determined in PBMCs of tamarins by NK cytotoxic assay. **c** The vRNAs were detected in plasma by real-time PCR

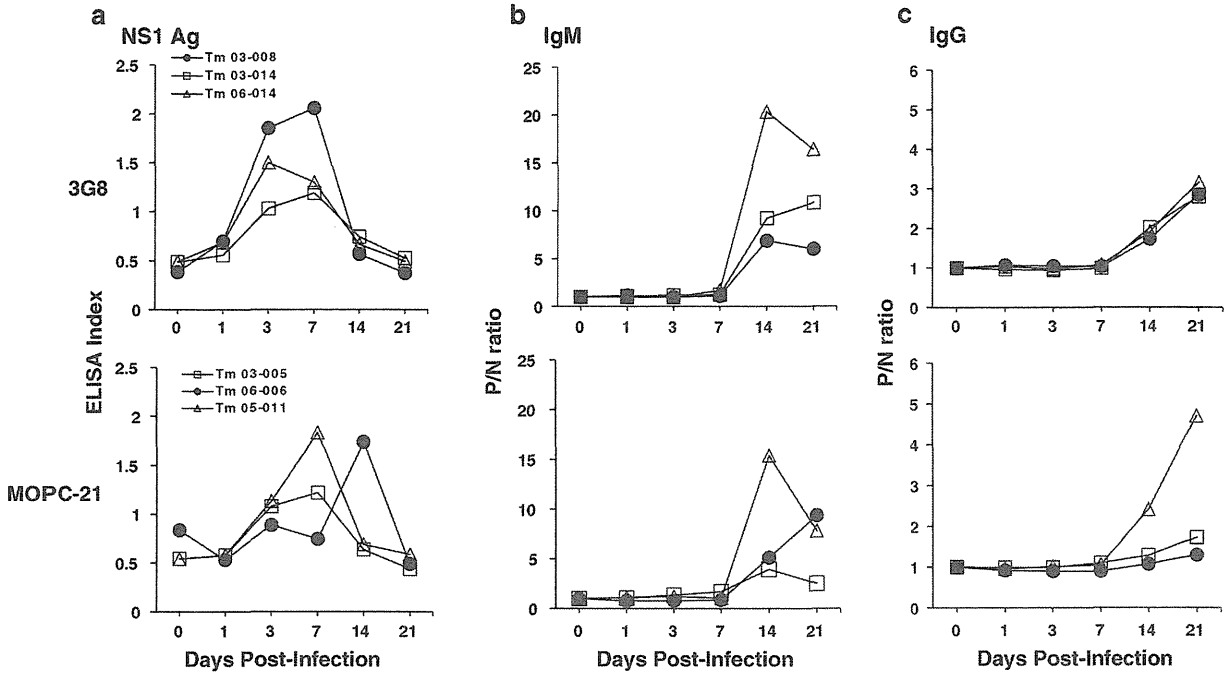

Fig. 3 Levels of NS1 antigen and DENV-specific IgM and IgG in plasma samples from DENV-infected tamarins after treatment with 3G8 or MOPC-21 mAb. The levels of NS1 antigen and DENV-specific IgM and IgG in plasma were measured by ELISA. **a** ELISA index of NS1 antigen, **b** positive/negative (P/N) ratio of DENV-specific IgM, **c** P/N ratio of DENV-specific IgG in plasma samples from DENV-infected tamarins after administration of the 3G8 or MOPC-21 mAb. The P/N ratio was calculated as the optical density of the test sample divided by that of a negative sample. P/N ratios <2 and ≥2 were considered to be negative and positive, respectively. Top, 3G8; bottom, MOPC-21 mAb

NK cells in tamarins and found that the depletion of $CD16^+$ NK cells had almost no effect on DENV replication (Fig. 2), indicating that this NK subpopulation is unlikely to contribute to controlling DENV replication. Interestingly, these results imply that the $CD16^-$ NK subpopulation may have a critical role of controlling DENV infection *in vivo*.

Using our model, we investigated the role of NK cells *in vivo* against DENV infection, which remains to be elucidated in several aspects. We previously reported that almost complete *in vivo* depletion of the $CD16^+$ NK subpopulation was not able to completely remove the NK-mediated cytotoxic activity in tamarins [29]. In this study, despite a transient but substantial reduction in the $CD16^+$ NK cell number following 3G8 treatment in tamarins, DENV replication was comparable to that in monkeys that received the control mAb. The NK-mediated cytotoxic activity was augmented in both study groups, indicating that $CD16^-$ NK cells were responsible for the cytotoxic activity and suggesting that they might play a role in controlling DENV replication.

The next question is how $CD16^-$ NK cells may regulate DENV infection. One possibility regarding $CD16^-$ NK cells is that $CD56^+$ or $CD57^+$ NK cells are involved in controlling DENV infection. Human NK cells are classically divided into two functional subsets based on their cell-surface density of CD56 and CD16, i.e., $CD56^{bright}CD16^-$ immunoregulatory cells and $CD56^{dim}CD16^+$ cytotoxic cells. Both subsets have been characterized extensively regarding their different functions, phenotypes, and tissue localization [8]. The NK cell number is maintained by a continuous differentiation process associated with the expression of CD57 that results in NK cells with poor responsiveness to cytokine stimulation but high cytolytic capacity [3, 18]. The second possibility is that $CD16^-$ NK cells have a non-cytolytic helper function. Generally, it is well known that NK cells possess both a cytolytic and a non-cytolytic helper function. It has been suggested that cytokine production is carried out by $CD56^{bright}CD16^-$ NK cells [4–6]. Interferon (IFN)-γ secreted by NK cells has shown potent antiviral effects against DENV infection in early phases [25]. One aspect of the NK helper function arises from recent evidence indicating that NK cells can be induced to function as non-cytotoxic helper cells following stimulation with interleukin-18 [19]. This cytokine induces IFN-γ secretion from NK cells and thus enables dendritic cells (DCs) to secrete IL-12, leading to Th1 polarization [19]. It is possible that $CD16^-$ NK cells, which have poor

cytotoxic activity but an enhanced ability to secrete cytokines and then lead to a Th1 response, are preserved during 3G8 administration. The persistence of this minor $CD16^-$ NK cell subpopulation could exert an antiviral effect through INF-γ-mediated pathways despite the depletion of $CD16^+$ NK cells. The third possibility is that $CD16^+$ NK cells of tamarins play pivotal roles against bacterial infections and cancer progression but not DENV-infected cells. We will address these possibilities for the roles of the NK subpopulation in the future studies.

In conclusion, this study provides a DENV *in vivo* replication model in tamarins and new information on the possible role of $CD16^+$ NK cells in DENV replication *in vivo*. It remains elusive whether the $CD16^+$ and $CD16^-$ NK subpopulations could play an important role in the control of primary DENV infection.

Acknowledgments We would like to give special thanks to members of the Corporation for Production and Research of Laboratory Primates for technical assistance. We also would like to give special thanks to Ms. Tomoko Ikoma and Ms. Mizuho Fujita for technical assistance. Moreover, we appreciate Dr. Keith A. Reimann (the NIH Nonhuman Primate Reagent Resource R24 RR016001, NIAID contact HHSN272200900037C) for providing CD16 antibody. This work was supported by grants from the Ministry of Health, Labor and Welfare of Japan (to Hirofumi Akari and Ichiro Kurane). This research was also supported by the Environment Research and Technology Development Fund (D-1007) from the Ministry of the Environment of Japan (to Tomoyuki Yoshida and Hirofumi Akari).

Conflict of interest The authors declare that the research was conducted in the absence of any commercial or financial relationships that could be construed as a potential conflict of interest.

References

1. Alcon-LePoder S, Sivard P, Drouet MT, Talarmin A, Rice C, Flamand M (2006) Secretion of flaviviral non-structural protein NS1: from diagnosis to pathogenesis. Novartis Found Symp 277:233–247 (discussion 247–253)
2. Azeredo EL, De Oliveira-Pinto LM, Zagne SM, Cerqueira DI, Nogueira RM, Kubelka CF (2006) NK cells, displaying early activation, cytotoxicity and adhesion molecules, are associated with mild dengue disease. Clin Exp Immunol 143:345–356
3. Bjorkstrom NK, Riese P, Heuts F, Andersson S, Fauriat C, Ivarsson MA, Bjorklund AT, Flodstrom-Tullberg M, Michaelsson J, Rottenberg ME, Guzman CA, Ljunggren HG, Malmberg KJ (2010) Expression patterns of NKG2A, KIR, and CD57 define a process of CD56dim NK-cell differentiation uncoupled from NK-cell education. Blood 116:3853–3864
4. Caligiuri MA (2008) Human natural killer cells. Blood 112: 461–469
5. Cooper MA, Fehniger TA, Turner SC, Chen KS, Ghaheri BA, Ghayur T, Carson WE, Caligiuri MA (2001) Human natural killer cells: a unique innate immunoregulatory role for the CD56(bright) subset. Blood 97:3146–3151
6. Farag SS, Caligiuri MA (2006) Human natural killer cell development and biology. Blood Rev 20:123–137
7. Fleit HB, Wright SD, Unkeless JC (1982) Human neutrophil Fc gamma receptor distribution and structure. Proc Natl Acad Sci USA 79:3275–3279
8. Gayoso I, Sanchez-Correa B, Campos C, Alonso C, Pera A, Casado JG, Morgado S, Tarazona R, Solana R (2011) Immunosenescence of human natural killer cells. J Innate Immun 3:337–343
9. Green S, Pichyangkul S, Vaughn DW, Kalayanarooj S, Nimmannitya S, Nisalak A, Kurane I, Rothman AL, Ennis FA (1999) Early CD69 expression on peripheral blood lymphocytes from children with dengue hemorrhagic fever. J Infect Dis 180:1429–1435
10. Guzman MG, Kouri G, Valdes L, Bravo J, Alvarez M, Vazques S, Delgado I, Halstead SB (2000) Epidemiologic studies on Dengue in Santiago de Cuba, 1997. Am J Epidemiol 152: 793–799 (discussion 804)
11. Halstead SB, Lan NT, Myint TT, Shwe TN, Nisalak A, Kalyanarooj S, Nimmannitya S, Soegijanto S, Vaughn DW, Endy TP (2002) Dengue hemorrhagic fever in infants: research opportunities ignored. Emerg Infect Dis 8:1474–1479
12. Halstead SB (2007) Dengue. Lancet 370:1644–1652
13. Hershkovitz O, Rosental B, Rosenberg LA, Navarro-Sanchez ME, Jivov S, Zilka A, Gershoni-Yahalom O, Brient-Litzler E, Bedouelle H, Ho JW, Campbell KS, Rager-Zisman B, Despres P, Porgador A (2009) NKp44 receptor mediates interaction of the envelope glycoproteins from the West Nile and dengue viruses with NK cells. J Immunol 183:2610–2621
14. Kurane I, Hebblewaite D, Ennis FA (1986) Characterization with monoclonal antibodies of human lymphocytes active in natural killing and antibody-dependent cell-mediated cytotoxicity of dengue virus-infected cells. Immunology 58:429–436
15. Lee SH, Miyagi T, Biron CA (2007) Keeping NK cells in highly regulated antiviral warfare. Trends Immunol 28:252–259
16. Libraty DH, Young PR, Pickering D, Endy TP, Kalayanarooj S, Green S, Vaughn DW, Nisalak A, Ennis FA, Rothman AL (2002) High circulating levels of the dengue virus nonstructural protein NS1 early in dengue illness correlate with the development of dengue hemorrhagic fever. J Infect Dis 186:1165–1168
17. Libraty DH, Acosta LP, Tallo V, Segubre-Mercado E, Bautista A, Potts JA, Jarman RG, Yoon IK, Gibbons RV, Brion JD, Capeding RZ (2009) A prospective nested case-control study of Dengue in infants: rethinking and refining the antibody-dependent enhancement dengue hemorrhagic fever model. PLoS Med 6:e1000171
18. Lopez-Verges S, Milush JM, Pandey S, York VA, Arakawa-Hoyt J, Pircher H, Norris PJ, Nixon DF, Lanier LL (2010) CD57 defines a functionally distinct population of mature NK cells in the human CD56dimCD16+ NK-cell subset. Blood 116:3865–3874
19. Mailliard RB, Alber SM, Shen H, Watkins SC, Kirkwood JM, Herberman RB, Kalinski P (2005) IL-18-induced CD83+CCR7+ NK helper cells. J Exp Med 202:941–953
20. Mathew A, Rothman AL (2008) Understanding the contribution of cellular immunity to dengue disease pathogenesis. Immunol Rev 225:300–313
21. Navarro-Sanchez E, Despres P, Cedillo-Barron L (2005) Innate immune responses to dengue virus. Arch Med Res 36:425–435
22. Omatsu T, Moi ML, Hirayama T, Takasaki T, Nakamura S, Tajima S, Ito M, Yoshida T, Saito A, Katakai Y, Akari H, Kurane I (2011) Common marmoset (Callithrix jacchus) as a primate model of dengue virus infection: development of high levels of viremia and demonstration of protective immunity. J Gen Virol 92:2271–2280. doi:10.1099/vir.0.031229-0
23. Scalzo AA, Corbett AJ, Rawlinson WD, Scott GM, Degli-Esposti MA (2007) The interplay between host and viral factors in shaping the outcome of cytomegalovirus infection. Immunol Cell Biol 85:46–54
24. Shresta S, Kyle JL, Robert Beatty P, Harris E (2004) Early activation of natural killer and B cells in response to primary dengue virus infection in A/J mice. Virology 319:262–273

25. Suwannasaen D, Romphruk A, Leelayuwat C, Lertmemongkolchai G (2010) Bystander T cells in human immune responses to dengue antigens. BMC Immunol 11:47
26. Vaughn DW, Green S, Kalayanarooj S, Innis BL, Nimmannitya S, Suntayakorn S, Endy TP, Raengsakulrach B, Rothman AL, Ennis FA, Nisalak A (2000) Dengue viremia titer, antibody response pattern, and virus serotype correlate with disease severity. J Infect Dis 181:2–9
27. Wahid SF, Sanusi S, Zawawi MM, Ali RA (2000) A comparison of the pattern of liver involvement in dengue hemorrhagic fever with classic dengue fever. Southeast Asian J Trop Med Public Health 31:259–263
28. Woollard DJ, Haqshenas G, Dong X, Pratt BF, Kent SJ, Gowans EJ (2008) Virus-specific T-cell immunity correlates with control of GB virus B infection in marmosets. J Virol 82:3054–3060
29. Yoshida T, Saito A, Iwasaki Y, Iijima S, Kurosawa T, Katakai Y, Yasutomi Y, Reimann KA, Hayakawa T, Akari H (2010) Characterization of natural Killer cells in tamarins: a technical basis for studies of innate immunity. Front Microbiol 1:128. doi: 10.3389/fmicb.2010.00128

Suppressor of Cytokine Signaling 1 DNA Administration Inhibits Inflammatory and Pathogenic Responses in Autoimmune Myocarditis

Kazuko Tajiri,*,† Kyoko Imanaka-Yoshida,‡,§ Akihiro Matsubara,*,¶ Yusuke Tsujimura,* Michiaki Hiroe,‖ Tetsuji Naka,# Nobutake Shimojo,† Satoshi Sakai,† Kazutaka Aonuma,† and Yasuhiro Yasutomi*,¶

Myocarditis and subsequent dilated cardiomyopathy are major causes of heart failure in young adults. Myocarditis in humans is highly heterogeneous in etiology. Recent studies have indicated that a subgroup of myocarditis patients may benefit from immune-targeted therapies, because autoimmunity plays an important role in myocarditis as well as contributing to the progression to cardiomyopathy and heart failure. Suppressor of cytokine signaling (SOCS) 1 plays a key role in the negative regulation of both TLR- and cytokine receptor-mediated signaling, which is involved in innate immunity and subsequent adaptive immunity. In this study, we investigated the therapeutic effect of SOCS1 DNA administration on experimental autoimmune myocarditis (EAM) in mice. EAM was induced by s.c. immunization with cardiac-specific peptides derived from α myosin H chain in BALB/c mice. In contrast to control myocarditis mice, SOCS1 DNA-injected mice were protected from development of EAM and heart failure. SOCS1 DNA administration was effective for reducing the activation of autoreactive CD4$^+$ T cells by inhibition of the function of Ag-presenting dendritic cells. Our findings suggest that SOCS1 DNA administration has considerable therapeutic potential in individuals with autoimmune myocarditis and dilated cardiomyopathy. ***The Journal of Immunology*****, 2012, 189: 2043–2053.**

Dilated cardiomyopathy (DCM) is a potentially lethal disorder of various etiologies for which no treatment is currently satisfactory (1); it often results from enteroviral myocarditis (2, 3). Many patients show heart-specific autoantibodies (3, 4), and immunosuppressive therapy can improve cardiac function in DCM patients who show no evidence of viral or bacterial genomes in heart biopsy samples (5). These observations suggest that autoimmunity plays an important role in myocarditis as well as contributing to the progression to cardiomyopathy and heart failure (6).

Experimental autoimmune myocarditis (EAM) is a model of postinfectious myocarditis and cardiomyopathy (7). A number of proinflammatory cytokines, including IL-1β, IL-6, IL-12, TNF-α, and GM-CSF, have been shown to contribute to the development of autoimmune myocarditis in animal models and human cases (8–13). EAM is a CD4$^+$ T cell-mediated disease (7, 14), and activation of self-Ag–loaded dendritic cells (DCs) is critical for expansion of autoreactive CD4$^+$ T cells. Activation of TLRs and IL-1 type 1 receptor and their common downstream signaling adaptor molecule, MyD88, in self-Ag–presenting DCs is also critical for the development of EAM (11, 15, 16). Compared with inhibition of a single cytokine, a more effective treatment might be inhibition of various signaling pathways to induce production of cytokines through both innate and adaptive immunity. One strategy that could accomplish this would be to target shared cytokine and TLR signal transduction pathways using suppressor of cytokine signaling (SOCS) molecules.

Recent lines of evidence indicate that SOCS proteins, originally identified as negative-feedback regulators in cytokine signaling, are involved in the regulation of TLR-mediated immune responses (17, 18). The SOCS family is composed of eight members: cytokine-inducible Src homology 2 domain-containing protein and SOCS1 to SOCS7 (19, 20). SOCS1 plays a key role in the negative regulation of both TLR-mediated signaling and cytokine receptor-mediated signaling, which are involved in innate immunity and subsequent adaptive immunity (21). The expression of SOCS1 is induced by various cytokines, including IFN-γ, IL-4, and IL-6, and also by TLR ligands, such as LPS and CpG-DNA (22). Several studies have demonstrated that SOCS1 is a negative regulator of LPS-induced macrophage activation and plays an essential role in suppression of systemic autoimmunity mediated by DCs (23–25). Thus, SOCS1 regulates not only adaptive immunity

*Laboratory of Immunoregulation and Vaccine Research, Tsukuba Primate Research Center, National Institute of Biomedical Innovation, Tsukuba, Ibaraki 305-0843, Japan; †Department of Cardiovascular Medicine, Majors of Medical Sciences, Graduate School of Comprehensive Human Sciences, University of Tsukuba, Tsukuba, Ibaraki 305-8575, Japan; ‡Department of Pathology and Matrix Biology, Mie University Graduate School of Medicine, Tsu, Mie 514-8507, Japan; §Mie University Matrix Biology Research Center, Mie University Graduate School of Medicine, Tsu, Mie 514-8507, Japan; ¶Division of Immunoregulation, Department of Molecular and Experimental Medicine, Mie University Graduate School of Medicine, Tsu, Mie 514-8507, Japan; ‖Department of Cardiology, National Center for Global Health and Medicine, Shinjuku, Tokyo 162-8655, Japan; and #Laboratory of Immune Signal, National Institute of Biomedical Innovation, Ibaragi, Osaka 565-0871, Japan

Received for publication December 13, 2011. Accepted for publication June 5, 2012.

This work was supported by Health Science Research grants from the Ministry of Health, Labor and Welfare of Japan and the Ministry of Education, Culture, Sports, Science and Technology of Japan.

Address correspondence and reprint requests to Dr. Yasuhiro Yasutomi, Laboratory of Immunoregulation and Vaccine Research, Tsukuba Primate Research Center, National Institute of Biomedical Innovation, 1-1 Hachimandai, Tsukuba, Ibaraki 305-0843, Japan. E-mail address: yasutomi@nibio.go.jp

The online version of this article contains supplemental material.

Abbreviations used in this article: BMDC, bone marrow-derived dendritic cell; DC, dendritic cell; dnSOCS1, dominant-negative suppressor of cytokine signaling 1; EAM, experimental autoimmune myocarditis; FS, fractional shortening; KO, knockout; LV, left ventricular; LVEDd, left ventricular end-diastolic dimension; LVESd, left ventricular end-systolic dimension; MyHC-α, cardiac myosin-specific peptide; pdnSOCS1, plasmid vector encoding dominant-negative suppressor of cytokine signaling 1; pSOCS1, plasmid vector encoding suppressor of cytokine signaling 1; QRT-PCR, quantitative real-time RT-PCR; SOCS, suppressor of cytokine signaling.

www.jimmunol.org/cgi/doi/10.4049/jimmunol.1103610

but also innate immunity by suppressing hyperactivation of macrophages and DCs.

In this study, we describe the therapeutic effect of SOCS1 DNA administration using plasmid DNA encoding SOCS1 for EAM. SOCS1 DNA therapy reduces myocarditis by regulating DC populations during EAM.

Materials and Methods

Animals

BALB/c mice and CB17.SCID mice were purchased from CLEA Japan. We used 5–7-wk-old male mice. All animals were cared for according to ethical guidelines approved by the Institutional Animal Care and Use Committee of the National Institute of Biomedical Innovation.

Immunization protocols

Mice were immunized with 100 μg cardiac myosin-specific peptide (MyHC-$\alpha_{614-629}$) Ac-RSLKLMATLFSTYASADR-OH (Toray Research Center) emulsified 1:1 in PBS/CFA (1 mg/ml; H37Ra; Sigma-Aldrich) on days 0 and 7 as described previously (12). For DC immunization, bone marrow-derived DCs (BMDCs) were generated as described (26). BMDCs were pulsed overnight with 10 μg/ml MyHC-α peptide and stimulated for another 4 h with 0.1 μg/ml LPS (Sigma-Aldrich) and 5 μg/ml anti-CD40 (BD Pharmingen) (15). Recipient mice received 2.5×10^5 pulsed and activated BMDCs i.p. on days 0, 2, and 4 and were killed 10 d after the first injection.

Plasmid construction and DNA transfection

Mouse SOCS1 cDNA and dominant-negative SOCS1 (dnSOCS1) cDNA were subcloned into the mammalian vector pcDNA3.1-myc/His(-) using oligonucleotide primers containing restriction sites for XhoI and EchoRI at the 5′ and 3′ ends, respectively. MyHC-α/CFA-immunized mice were injected i.p. with 100 μg of plasmid DNA in 200 μl PBS on days 0, 5, and 10. BMDC-transferred mice and $CD4^+$ T cell adoptive-transferred SCID mice were treated with plasmid DNA on days 0 and 5.

Histopathologic examination

Myocarditis severity was scored on H&E-stained sections using grades from 0–4: 0, no inflammation; 1, <25% of the heart section involved; 2, 25–50%; 3, 50–75%; and 4, >75%. To quantify the fibrotic area, ventricular sections were stained with Sirius Red. The fibrotic area was calculated as the sum of all areas stained positive for Sirius Red divided by the sum of all myocardial areas in each mouse. Two independent researchers scored the slides separately in a blinded manner.

Flow cytometry

Heart inflammatory cells were isolated and processed as described (15, 27). Cells were stained using fluorochrome-conjugated mouse-specific Abs against CD45, CD4, CD3e, CD44, CD62L, and CD40L (BD Biosciences). Samples were analyzed on an FACSCalibur cell sorter (BD Biosciences).

Measurements of cytokines and chemokines

Hearts were homogenized in media containing 2.5% FBS. Supernatants were collected after centrifugation and stored at −80°C. For in vitro stimulation assay of primary $CD4^+$ T cells, naive $CD4^+CD62L^+$ T cells were isolated from the spleens by MACS ($CD4^+CD62L^+$ T Cell Isolation Kit II; Miltenyi Biotec). A total of 1.5×10^7 $CD4^+CD62L^+$ cells were then stimulated with recombinant mouse IL-2 (R&D Systems) or recombinant mouse IL-12 (R&D Systems). Concentrations of cytokines and chemokines in the heart homogenates or culture supernatants were measured with Quantikine ELISA kits (R&D Systems).

Proliferative responses of T cells

Proliferation of T cells was assessed as previously described (28). Briefly, mice were immunized as described above, and the spleens collected on day 14. Cells were cultured with 5 μg/ml MyHC-α for 72 h and pulsed with 0.5 μCi [^{3}H]thymidine 8 h before being measured with a β counter. For in vitro stimulation assay of primary $CD4^+$ T cells, naive $CD4^+CD62L^+$ T cells were isolated from the spleens by MACS ($CD4^+CD62L^+$ T Cell Isolation Kit II; Miltenyi Biotec). A total of 10^5 $CD4^+CD62L^+$ cells were then stimulated with 5 μg/ml anti-CD3ε, 5 μg/ml anti-CD3ε, 1 μg/ml anti-CD28, 50 ng/ml PMA, and 500 ng/ml ionomycin or with 1 μg/ml Con A together with 0.25×10^5 DCs. Proliferative responses were assessed after 48 h in 2.5% RPMI 1640 medium by measurement of the [^{3}H]thymidine incorporation.

Western blot analysis

Total lysates from $CD4^+$ T cells or DCs were immunoblotted and probed with Abs directed against STAT1 (Santa Cruz Biotechnology) and p-STAT1 protein (Cell Signaling Technology). HRP-conjugated goat anti-rabbit IgG (Bio-Rad) was used to identify the binding sites of the primary Ab.

Adoptive transfer of T cells

Splenocytes were collected from diseased mice and cultured with 5 μg/ml MyHC-α for 48 h. A total of 5×10^6 $CD4^+$ T cells were purified by using anti-CD4 magnetic beads (Miltenyi Biotec) and injected i.p. into the SCID mice. The mice were killed 10 d after the injection.

Quantitative real-time RT-PCR

Total RNA was prepared using TRIzol reagent (Invitrogen) according to the manufacturer's instructions. cDNA was synthesized from 1 μg total RNA by reverse transcriptase (Takara). Quantitative real-time RT-PCR (QRT-PCR) analysis was performed with LightCycler (Roche Diagnostics). Primers for mouse *Socs1* were 5′-GTGGTTGTGGAGGGTGAGAT-3′ (sense) and 5′-CCTGAGAGGTGGGATGAGG-3′ (antisense). Primers for mouse *Hprt* were 5′-TCCTCCTCAGACCGCTTTT-3′ (sense) and 5′-CCTGGTTCATCATCGCTAATC-3′ (antisense). Data were normalized by the level of *Hprt* expression in each sample.

Echocardiography

Transthoracic echocardiography was performed on animals on day 35 by using a Prosound α6 with a 10-MHz transducer (Aloka). The left ventricular (LV) chamber dimensions were measured from the M-mode. Two independent investigators who conducted the echocardiography were unaware of the treatment status.

Statistical analysis

All data were expressed as means ± SEM. Statistical analyses were performed using the two-tailed *t* test or Mann–Whitney *U* test for experiments comparing two groups. The *p* values <0.05 were considered statistically significant.

Results

SOCS1 DNA administration inhibits the development of EAM

To examine the effect of in vivo gene delivery of *Socs1* on the pathogenesis of EAM, BALB/c mice were injected with a mammalian expression plasmid vector encoding SOCS1 (pSOCS1) during the course of EAM induction (Fig. 1A). QRT-PCR analysis revealed elevated expression of *Socs1* in the control EAM heart (Fig. 1B). Importantly, in the SOCS1 DNA-administered mice, *Socs1* was strongly expressed in the heart. By day 28, *Socs1* gene expression was significantly elevated in the pSOCS1-treated heart as compared with the controls (Supplemental Fig. 1). Gross cardiac enlargement and edema were reduced in mice with EAM that received pSOCS1 as compared with those in control empty plasmid DNA-administered EAM mice (Fig. 1C). The heart-to-body weight ratio in the pSOCS1-injected mice was significantly decreased as compared with that in the control plasmid-administered mice (Fig. 1D). The pSOCS1-injected EAM mice had a significantly lower myocarditis severity score and fewer infiltrating inflammatory cells than did the control plasmid-injected mice (Fig. 1E–G). The empty vector [pcDNA3.1-myc/His(-)] was used as the control and did not have any effects on EAM in our experiments (data not shown).

Recently, Hanada et al. (29) demonstrated that dnSOCS1, which has a point mutation (F59D) in a functionally critical kinase inhibitory region of SOCS1, strongly augmented cytokine-dependent JAK-STAT activation both in vivo and in vitro as an antagonist of SOCS1. We examined the effect of dnSOCS1 on the clinical course of EAM. Mice administered a plasmid vector

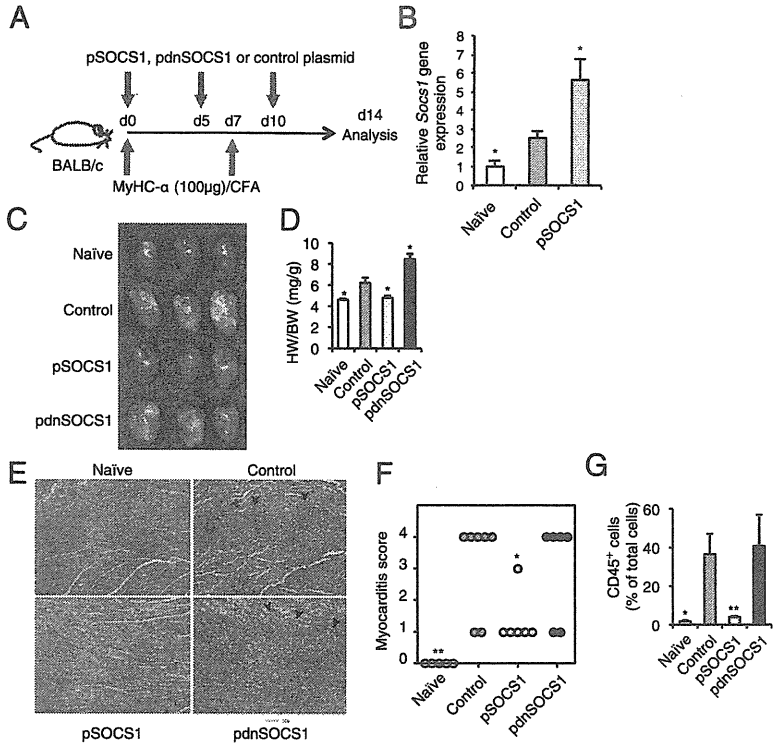

FIGURE 1. Amelioration of EAM and heart failure by SOCS1 DNA administration. (**A**) BALB/c mice were immunized twice, on days 0 and 7, with 100 μg of MyHC-α and treated with pSOCS1, pdnSOCS1, or control plasmid on days 0, 5, and 10. (**B**) QRT-PCR for the *Socs1* gene. RNA samples were obtained from hearts of immunized mice on day 14 and used as a template for QRT-PCR. Results represent the average gene induction in five independent heart samples. (**C**) Representative gross hearts (day 14) of naive and EAM mice treated with the indicated plasmid. (**D**) Heart-to-body weight ratios of naive and EAM mice with indicated treatment (n = 5 mice/group). (**E**) Representative H&E-stained sections of hearts from naive and immunized mice. Arrowheads indicate infiltrating cells. Scale bar, 50 μm. (**F**) Myocarditis severity in heart sections stained with H&E (n = 5–7 mice/group). (**G**) Flow cytometry analysis of $CD45^+$ heart infiltrates of naive and immunized mice (n = 5–7 mice/group). Data are representative of at least two independent experiments. Error bars represent means ± SEM. $*p < 0.05$, $**p < 0.01$ compared with control.

encoding dnSOCS1 (pdnSOCS1) showed augmentation of gross heart enlargement, edema, and heart-to-body weight ratio (Fig. 1C, 1D). However, the myocardial leukocyte infiltration and myocarditis scores were not significantly different between the pdnSOCS1- and control plasmid-administered mice (Fig. 1E–G).

To clarify the adverse effect of dnSOCS1 DNA administration on the development of EAM, we used mice immunized with a tithe amount (10 μg) of MyHC-α instead of the usual amount of peptide for EAM development (Fig. 2A). Those MyHC-α–immunized mice injected with the control plasmid or pSOCS1 did not develop myocarditis (Fig. 2B–F). However, immunized mice injected with pdnSOCS1 developed myocarditis with inflammatory infiltrates (Fig. 2B–F). Thus, administration of pSOCS1 is effective against the development of EAM, and the inhibition of SOCS1 by use of a SOCS1 antagonist adversely affects myocarditis.

SOCS1 DNA administration prevents progression of heart failure and fibrosis after myocarditis

Some patients diagnosed with myocarditis after viral, bacterial, or protozoal infection develop heart failure (2). On day 35 of the present experiment, mice immunized with MyHC-α showed increased LV end-diastolic dimensions (LVEDd) and LV end-systolic dimensions (LVESd) and decreased fractional shortening (FS); however, pSOCS1-injected mice showed almost normal chamber size and LV function (Fig. 3A, 3B). In contrast, LV dysfunction and chamber dilatation in pdnSOCS1-administered mice were manifested as significant increases in LVEDd and LVESd and decrease in FS (Fig. 3A, 3B). In these EAM models, on day 35, hearts from myocarditis mice showed interstitial fibrosis without active leukocyte infiltration. The fibrotic area in mice administered pSOCS1 was significantly smaller than that in control plasmid-injected mice (Fig. 3C, 3D). Although pdnSOCS1-injected mice developed severe cardiac fibrosis, the difference between the fibrotic areas in pdnSOCS1- and control plasmid-injected mice was not statistically significant (Fig. 3C, 3D). These inhibitory effects of pSOCS1 on the development of fibrosis and heart failure were considered to be the result of inhibition of myocardial inflammation because myocarditis developed mice injected with pSOCS1 on day 14, 21, and 28 did not show inhibitory effects on fibrosis and heart failure (data not shown).

Cardiac myosin-specific $CD4^+$ T cell response and cytokine production

Autoimmune myocarditis is a $CD4^+$ T cell-mediated disease (7, 15). Proliferative responses of $CD4^+$ T cells after in vitro restimulation with MyHC-α were not clearly seen in pSOCS1-injected mice; however, the proliferation of $CD4^+$ T cells from pdnSOCS1-injected mice was enhanced (Fig. 4A). Production of IL-2, IL-6, IL-10, IL-17, IL-22, IFN-γ, TNF-α, CCL2, CCL3, CCL5, CCL17, and CXCL10 by $CD4^+$ T cells from EAM mice was enhanced by in vitro restimulation with the MyHC-α epitope peptide. This cardiac-Ag–specific cytokine production by $CD4^+$ T cells was decreased in the supernatants of in vitro MyHC-α–restimulated $CD4^+$ T cells from pSOCS1-administered mice but

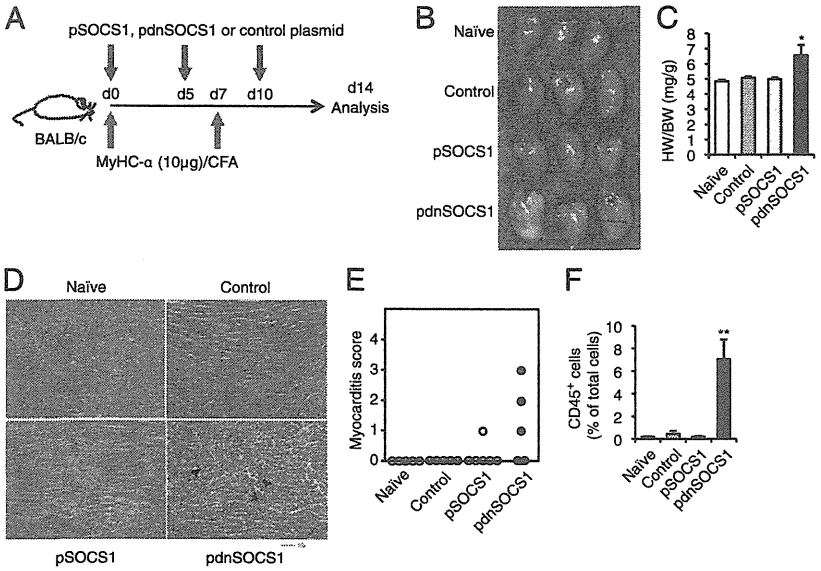

FIGURE 2. Increased susceptibility to EAM induced by inhibition of SOCS1. (**A**) Mice were immunized twice, on days 0 and 7, with 10 μg of MyHC-α emulsified 1:1 in PBS/CFA and treated with pSOCS1, pdnSOCS1, or control plasmid on days 0, 5, and 10. (**B**) Representative gross hearts (day 14) of naive and 10 μg of MyHC-α–immunized mice treated with the indicated plasmid. (**C**) Heart-to-body weight ratios of naive and immunized mice (n = 5 to 6 mice/group). (**D**) Representative H&E-stained sections of hearts from naive and immunized mice. Arrowheads indicate infiltrating cells. Scale bar, 50 μm. (**E**) Myocarditis severity in heart sections stained with H&E (n = 5 to 6 mice/group). (**F**) Flow cytometry analysis of $CD45^+$ heart infiltrates of naive and immunized mice (n = 5 mice/group). Data are representative of at least two independent experiments. Error bars represent means ± SEM. $*p < 0.05$, $**p < 0.01$ compared with control.

was increased in the supernatants of these cells from pdnSOCS1-administered mice (Fig. 4B). In contrast, cardiac-Ag–specific production of IL-1β, IL-10, and CXCL1 was not detected in the culture supernatants of in vitro-restimulated $CD4^+$ T cells from control plasmid-, pSOCS1-, or pdnSOCS1-injected mice (data not shown). Taken together, these results indicate that SOCS1 DNA

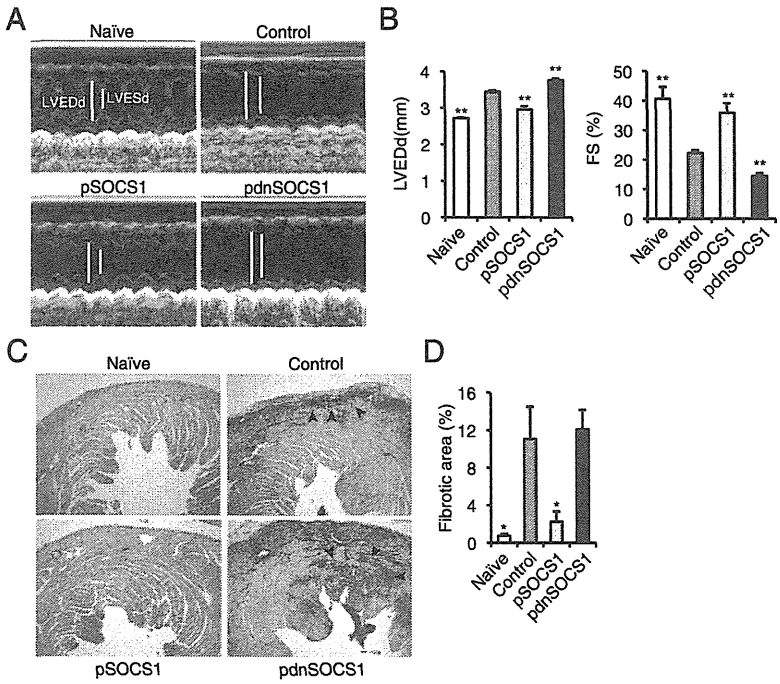

FIGURE 3. SOCS1 DNA administration prevents progression to heart failure. (**A** and **B**) Echocardiography was performed on naive and immunized mice on day 35. (A) Representative M-mode echocardiograms. Bars indicate LVESd and LVEDd. Bar graphs (B) represent LVEDd and percentage of FS from the indicated animals (n = 9 mice/group). The percentage FS was calculated according to the following formula: FS (%) = (LVEDd − LVESd)/LVEDd. (**C** and **D**) Heart tissue sections were stained with Sirius Red and analyzed for fibrosis at day 35. Representative Sirius Red-stained sections of hearts. Scale bar, 50 μm. (C) Arrowheads indicate fibrotic area. (D) The degree of fibrosis was calculated as the percentage of the fibrotic area in relation to the total heart area (n = 5 mice/group). Data are representative of at least two independent experiments. Error bars represent means ± SEM. $*p < 0.05$, $**p < 0.01$ compared with control.

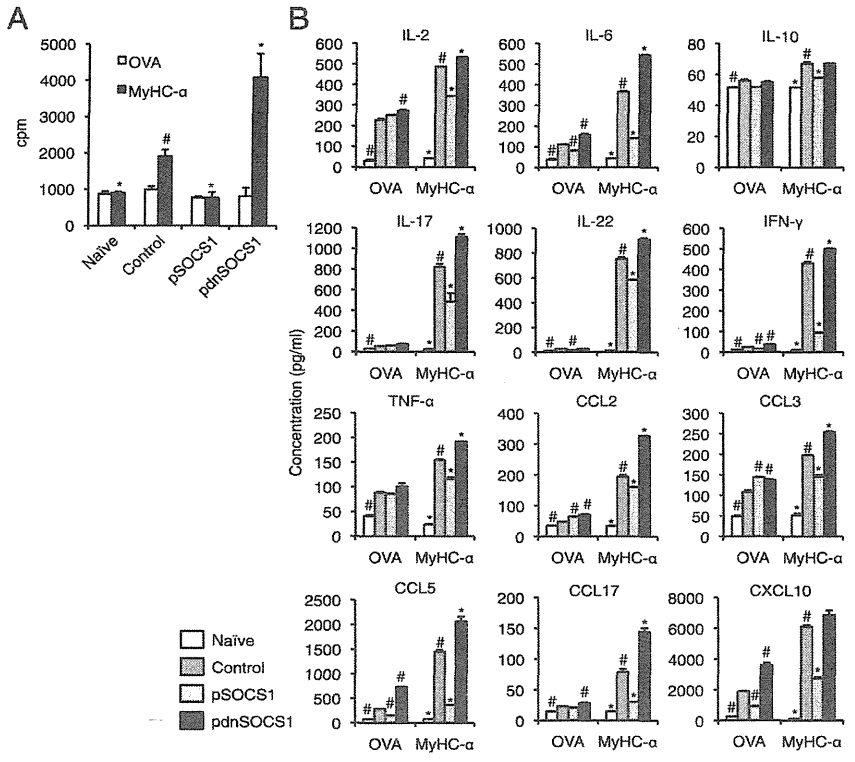

FIGURE 4. Impaired expansion of heart-specific $CD4^+$ T cells in pSOCS1-treated mice. (**A**) Splenocytes were isolated from naive and EAM mice treated with pSOCS1, pdnSOCS1, or control plasmid on day 14 and restimulated in vitro with MyHC-α or OVA peptide for 72 h. Proliferation was assessed by measurement of [^{3}H]thymidine incorporation. Data represent means ± SEM of triplicates from one of three independent experiments. (**B**) Cytokines and chemokines in the culture supernatants of splenocytes were measured by ELISA after 48 h of restimulation with MyHC-α or OVA peptide. Data are expressed as mean ± SEM from triplicate culture wells. Results of one of two representative experiments are shown. $^*p < 0.05$ compared with MyHC-α–stimulated control, $^\#p < 0.05$ compared with OVA-stimulated control.

delivery inhibits the activation of myosin-specific $CD4^+$ T cells and strongly suggest that impaired $CD4^+$ Th cell function prevents EAM development in pSOCS1-injected mice after immunization with cardiac self-Ag.

To evaluate whether pSOCS1 administration affects Ag-specific $CD4^+$ T cell function in other models, we injected plasmid DNA into an autoimmune gastritis model and an OVA-immunized model. In the autoimmune gastritis model, gastric-Ag–specific production of IL-2, IL-6, IL-13, IL-17, IL-22, IFN-γ, TNF-α, CCL2, CCL5, CCL17, and CXCL10 by $CD4^+$ T cells was decreased in pSOCS1-administered mice but increased in pdnSOCS1-administered mice (Supplemental Fig. 2). Lower amounts of cytokines (including IL-2, IL-6, IL-13, IFN-γ, TNF-α, CCL2, CCL3, CCL5, CCL17, and CXCL10) were also produced in $CD4^+$ T cells from pSOCS1-injected OVA-immunized mice (Supplemental Fig. 3). These results suggest that pSOCS1 administration may suppress Ag-specific $CD4^+$ T cell activation in various autoimmune diseases and foreign body infections.

SOCS1 DNA administration inhibits the production of proinflammatory cytokines and $CD4^+$ T cell differentiation in the heart

We also examined whether SOCS1 DNA administration has an effect on cytokine and chemokine milieu in the heart. On day 14 after MyHC-α immunization, heart homogenates from pSOCS1-injected mice had significantly decreased amounts of proinflammatory cytokines, including IL-1β and IL-6, and of myelotropic chemokines, including CCL5, CXCL1, and CXCL10 (Fig. 5A). In contrast, hearts from mice injected with pdnSOCS1 showed greatly increased amounts of proinflammatory cytokines and chemokines (Fig. 5A). SOCS1 protein has been shown to regulate T cell differentiation (17, 18). To determine the differentiation of $CD4^+$ T cells during EAM, we examined the heart-infiltrating $CD4^+$ T cell populations by FACS analysis. Activated $CD4^+$ T cells ($CD4^+CD40L^+$) and effector memory $CD4^+$ T cells ($CD44^+CD62L^-$) were reduced in the pSOCS1-injected mice (Fig. 5B). Thus, protection from EAM in pSOCS1-administered mice is associated with abrogation of proinflammatory cytokines, chemokines, and $CD4^+$ T cell differentiation in the heart.

SOCS1 DNA injection does not have a direct suppressive effect on $CD4^+$ T cell activation

To gain new insights into the mechanism of protection from myocarditis, we investigated whether pSOCS1 therapy directly affects $CD4^+$ T cell activation. Naive T cells ($CD4^+CD62L^+$ cells) were isolated from non-EAM mice injected with pSOCS1, pdnSOCS1, or control plasmid, and their primary responses to various stimuli were compared (Fig. 6A). As shown in Fig. 6B, there were no differences in IFN-γ–induced STAT1 activation among these $CD4^+$ T cells. There were also no differences in primary responses to stimulation with anti-CD3ε, anti-CD3ε/anti-CD28, PMA/ionomycin, or Con A presented by mitomycin C-treated wild-type DCs among pSOCS1-, pdnSOCS1-, and control plasmid-treated $CD4^+$ T cells (Fig. 6C). Chong et al. (30) demonstrated that SOCS1-deficient T cells produced substantially greater levels of IFN-γ in response to IL-2 or IL-12. From these findings, we assessed the production of IFN-γ from $CD4^+$ T cells by using the same experiments. In the culture supernatants of

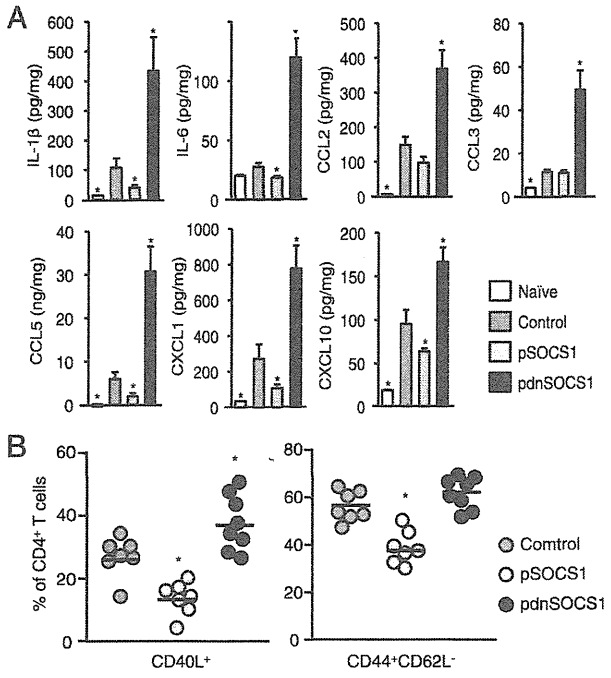

FIGURE 5. Cytokine and chemokine responses and $CD4^+$ T cell differentiation in the heart. (**A**) Myocardial tissues were homogenated and processed by ELISA to detect cytokines and chemokines on day 14. Bar graphs show group means ± SEM of 8–16 mice/group. Results of one of three representative experiments are shown. (**B**) Heart-infiltrating cells were isolated from EAM mice treated with indicated plasmid DNA. Cells were stained for CD4, CD40L, CD44, and CD62L. CD44 and CD62L expression are based on gates set from total $CD4^+$ T cells. Bar graphs show group means ± SEM of 5–9 mice/group. Data are representative of two independent experiments. $*p < 0.05$ compared with control.

$CD4^+$ T cells stimulated with IL-2 or IL-12, there were also no differences in IFN-γ production (Fig. 6D). These results indicate that in vivo administration of pSOCS1 does not directly affect $CD4^+$ T cell activation.

In vivo SOCS1 DNA administration inhibits DC function

Although $CD4^+$ T cell differentiation was inhibited in pSOCS1-treated mice (Fig. 5B), our results suggested that in vivo *Socs1* gene administration has no direct effect on $CD4^+$ T cell activation (Fig. 6). We therefore investigated whether in vivo pSOCS1 administration inhibits the function of Ag-presenting DCs by stimulation through the TLR pathway. DCs from mice administered pSOCS1, pdnSOCS1, or control plasmid were stimulated with LPS for 24 h (Fig. 7A). STAT1 phosphorylation was attenuated in DCs from pSOCS1-injected mice and enhanced in DCs from pdnSOCS1-injected mice (Fig. 7B). The production of proinflammatory cytokines, including IL-6, TNF-α, and IFN-γ, was inhibited in DCs from pSOCS1-injected mice and enhanced in DCs from pdnSOCS1-injected mice (Fig. 7C). These results indicate that in vivo administration of *Socs1* affects DC function. In the current study, the cardiac-Ag–specific proliferative response and cytokine production of $CD4^+$ T cells were inhibited in pSOCS1-injected EAM mice (Fig. 4). We next assessed the functional capability of DCs to prime and expand autoreactive $CD4^+$ T cells from mice injected with each plasmid as a measure of Ag-specific proliferative responses of $CD4^+$ T cells from MyHC-α–immunized mice. Myosin-specific $CD4^+$ T cells were cocultured with MyHC-α–pulsed DCs from pSOCS1-, pdnSOCS1-, and control plasmid-treated mice (Fig. 7D). Interestingly, the proliferative responses of $CD4^+$ T cells cocultured with DCs from pSOCS1-treated mice were much weaker than those of cells cultured with DCs from control plasmid-treated mice, and these proliferative responses of $CD4^+$ T cells were enhanced by coculturing with DCs from pdnSOCS1-administered mice (Fig. 7E). These results suggest that in vivo gene delivery of *Socs1* suppresses the functional capability of DCs to prime and expand autoreactive $CD4^+$ T cells.

SOCS1 DNA administration inhibits the development of myocarditis induced by cardiac myosin peptide-loaded BMDC transfer but not by $CD4^+$ T cell transfer

Functionally interposed SOCS1 is induced in various cell populations, including leukocytes, vascular cells, and cardiomyocytes (18, 31, 32). A mouse model of EAM was established by cell transfer using peptide-pulsed DCs or cardiac epitope-specific $CD4^+$ T cells (7, 14). The effects of pSOCS1 administration in mice transferred with $CD4^+$ T cells from mice with EAM were assessed. pSOCS1, pdnSOCS1, or control plasmid was injected into mice transferred with cardiac myosin-specific $CD4^+$ T cells (Fig. 8A). All mice transferred with $CD4^+$ T cells developed myocarditis, and no therapeutic effects were seen in pSOCS1-injected mice (Fig. 8B–D). Furthermore, pdnSOCS1 administration showed no adverse effect on the status of myocarditis induced by $CD4^+$ T cell transfer (Fig. 8B–D). These findings suggest that systemic injection of pSOCS1 is not effective for inhibition of autoreactive $CD4^+$ T cell activation and recruitment to the heart during myocarditis development. Next, we administered pSOCS1, pdnSOCS1, or control plasmid into mice transferred with MyHC-α–loaded BMDCs (Fig. 8E). Interestingly, pSOCS1 injection inhibited the development of myocarditis after MyHC-α–loaded BMDC transfer, and myocarditis deteriorated after administration of pdnSOCS1 (Fig. 8F–H). These results indicate that the therapeutic effects of SOCS1 DNA administration on EAM contribute to professional APCs such as DCs and also provide evidence for the potential utility of SOCS1 DNA inoculation as an approach to gene therapy for myocarditis.

Discussion

There have been no effective fundamental therapies for acute myocarditis; therefore, supportive care for LV dysfunction is the first line of treatment. Because patients generally present days to weeks after the initial viral infection, antiviral therapy has limited applicability in patients with acute viral myocarditis. The long-term sequelae of viral myocarditis appear to be related to abnormal cellular and humoral immunity; therefore, many clinicians believe that immunosuppression is beneficial for myocarditis treatment (2). In this study, we showed that administration of SOCS1 DNA is effective for inhibiting the development of EAM in BALB/c mice, suggesting a novel immunotherapy for myocarditis. To our knowledge, this is the first report showing that gene delivery of *Socs1* prevents autoimmune disease.

Animal models have greatly advanced our knowledge of the pathogenesis of myocarditis and inflammatory cardiomyopathy. Infection of BALB/c mice with either Coxsackievirus or murine CMV results in the development of acute myocarditis from days 7–14 postinfection that is characterized by myocyte damage due to viral cytotoxicity, and the infectious virus cannot be detected past day 14 of the infection (7). After elimination of viruses, mice showed autoimmune myocarditis, which is associated with mononuclear infiltration of the myocardium and production of autoantibodies to cardiac myosin (7), similar to the pathogenesis of autoimmune myocarditis in humans (3, 4, 33). These autoim-

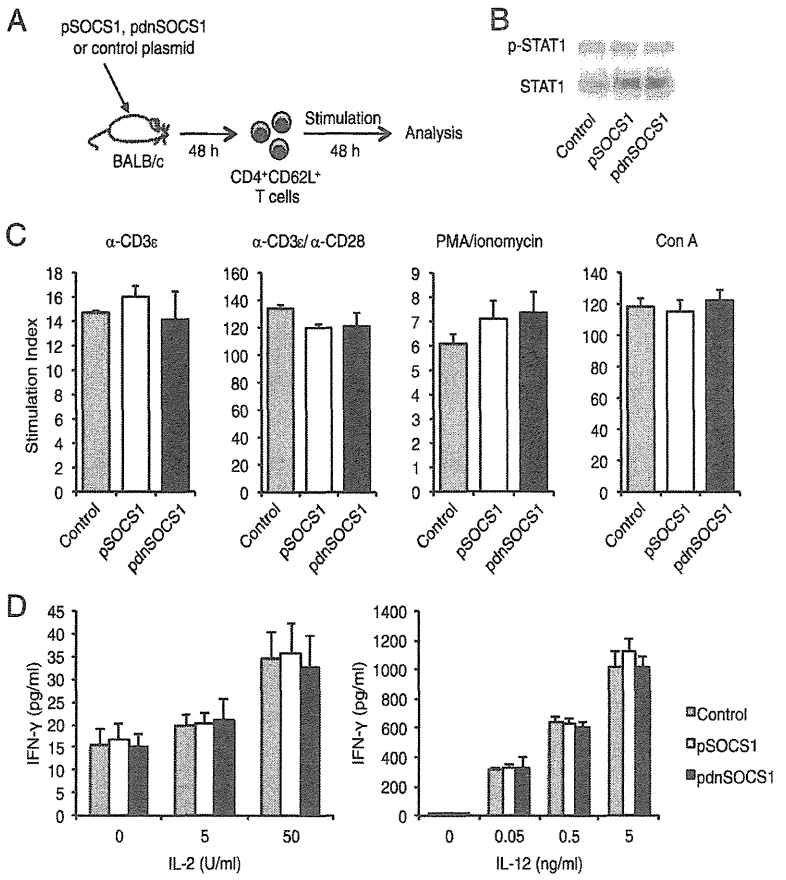

FIGURE 6. Primary responses of $CD4^+$ T cells from pSOCS1-, pdnSOCS1-, and control plasmid-treated mice. (**A**) $CD4^+CD62L^+$ T cells from mice injected with pSOCS1, pdnSOCS1, or control plasmid were stimulated with IFN-γ, anti-CD3ε, anti-CD3ε, anti-CD28, PMA/ionomycin, and Con A in the presence of wild-type DCs, IL-2, or IL-12. (**B**) STAT1 phosphorylation of $CD4^+$ T cells after IFN-γ treatment (10 ng/ml) was assessed by Western blotting. (**C**) T cell proliferation was measured after 48 h of culture. (**D**) IFN-γ in the culture supernatants was measured by ELISA. Values are expressed as means ± SEM of triplicate culture wells. Results of one of at least two representative experiments are shown.

mune responses are thought to be elicited by two mechanisms. One is molecular mimicry: responses to microbial Ags could result in the activation of T cells that are cross-reactive with self-Ags. Another possibility is bystander activation of autoreactive cells. APCs that have become activated in the inflammatory milieu of a pathogenic infection can stimulate the activation and proliferation of autoreactive T or B cells in a process known as bystander activation (reviewed in Ref. 34). Thus, immune responses to myocytes involving various innate and adaptive immune pathways were recognized during myocarditis development. The cardiac myosin peptide-immunized mouse EAM model reflects human autoimmune myocarditis and heart failure after elimination of infectious pathogens.

Recent studies have indicated that various microbes use the host's SOCS proteins for manipulating cytokine receptor signaling as one of the strategies to evade immune responses (35, 36). Coxsackievirus usually infects cardiomyocytes and induces the expression of SOCS1 and SOCS3 in cardiomyocytes, which can result in evasion of immune responses and facilitation of virus replication by inhibition of JAK–STAT signaling (32, 37). These findings indicate that it may be harmful to administer SOCS1 DNA in the acute phase of infectious myocarditis because it may augment viral replication by inhibition of IFN signaling. The effect of SOCS1 transduction on viral myocarditis has been examined by Yasukawa et al. (32). The SOCS1-transgenic mice infected with CVB3 showed increased myocardial injury, virus replication, and mortality. In contrast, they also showed that SOCS1 inhibition in the heart through adeno-associated virus-mediated expression of dnSOCS1 increased resistance to the acute cardiac injury caused by CVB3 infection. These results were acceptable because SOCS proteins have emerged as frequent targets of viral exploitation. Furthermore, when administrating JAK inhibitors, such as SOCS, active serious infections should have been resolved before the start of treatment. It is considered to be inappropriate to use JAK inhibitors for a person with infectious disease or their possibility with consideration for complication of infection (38–40). In contrast, the overactive autoimmune responses triggered by microbial pathogens can persist after elimination of infectious pathogens (7). Therefore, we examined the efficacy of SOCS1 transfection by using EAM induced by cardiac autoantigen immunization in the absence of viral infection. In the current study, we clearly showed the efficacy of *Socs1* gene transfer as an immunosuppressive therapy for myocarditis under infectious pathogen-free conditions in an EAM mice model. The results of a recent randomized, double-blind, placebo-controlled study showed that immunosuppressive therapy, including prednisone and azathioprine, was effective in patients with myocarditis and inflammatory cardiomyopathy and without evidence of the myocardial viral genome (41). These findings indicate that *Socs1* gene transfer can be effective to treat some clinical

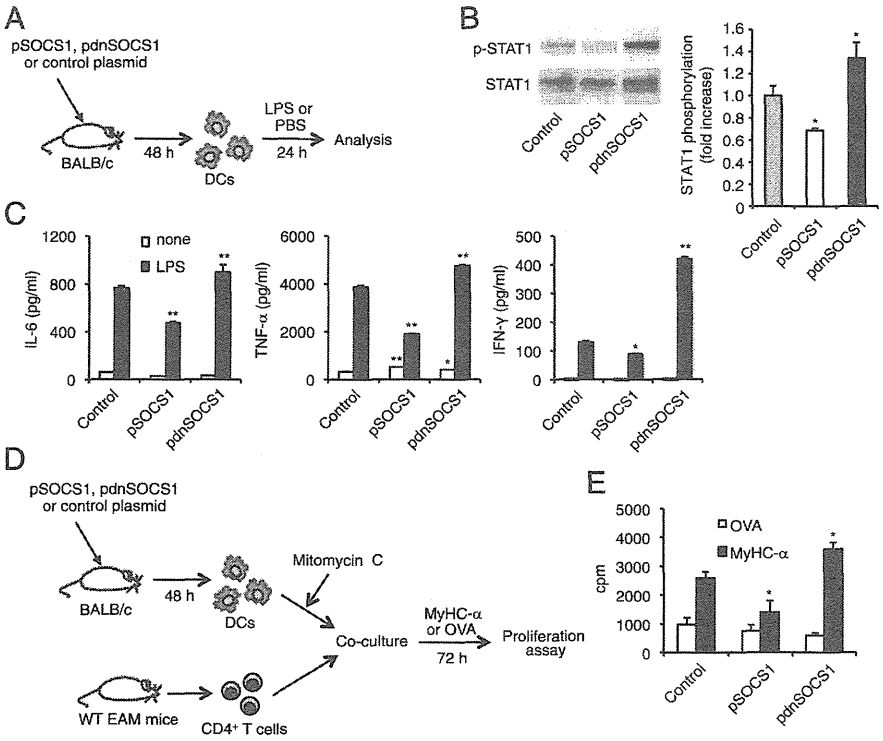

FIGURE 7. Functional capacities of DCs from pSOCS1-, pdnSOCS1-, and control plasmid-treated mice. (**A**) DCs from mice treated with pSOCS1, pdnSOCS1, or control plasmid were stimulated with LPS for 24 h. (**B**) STAT1 phosphorylation of DCs was assessed by Western blotting. Densitometry ratios of pSTAT1/STAT1 are shown as fold induction, the ratio for DCs from control plasmid-injected mice being set at 1. Results are means of five independent experiments ± SEM. Blots are representative of experiments performed a minimum of three times. (**C**) IL-6, TNF-α, and IFN-γ in the culture supernatants were measured by ELISA. Values indicate means ± SEM of triplicate culture wells from one of three independent experiments. (**D** and **E**) Heart-specific $CD4^+$ T cells from EAM mice were restimulated with MyHC-α or OVA peptide on DCs from mice treated with control plasmid, pSOCS1, or pdnSOCS1 for 72 h before measurement of [^{3}H]thymidine incorporation. Each value represents mean ± SEM cpm values of six different culture wells. Results of one of three representative experiments are shown. $*p < 0.05$, $**p < 0.01$ compared with control.

cases of myocarditis and inflammatory cardiomyopathy associated with autoimmunity and without the virus genome in the myocardium, as well as EAM in mice.

In the current study, we demonstrated that the administration of plasmid DNA encoding SOCS1 did not affect autoreactive $CD4^+$ T cell function (Fig. 6) and adoptive transfer of autoreactive $CD4^+$ T cells was able to induce myocarditis in SOCS1 DNA-administered SCID mice (Fig. 8A–D), suggesting that SOCS1 DNA does not suppress either $CD4^+$ T cell recruitment or accumulation of other inflammatory cells in the heart. In contrast, the introduced SOCS1 DNA inhibited the activation of DCs producing proinflammatory cytokines (Fig. 7C). In fact, inhibition of the phosphorylation of STAT1 molecules was observed in DCs from mice injected with SOCS1 DNA (Fig. 7B). In addition, the proliferative responses of $CD4^+$ T cells cocultured with DCs from pSOCS1-treated mice were much weaker than those of cells cultured with DCs from control plasmid-injected mice (Fig. 7E). These results suggest that the inoculated SOCS1 DNA may have been transfected into DCs and impaired DC function in vivo. Contrary to expectations, we could not find evidence of direct transfection of inoculated DNA into DCs in the heart, spleen, peritoneal cavity, or lymph nodes. Although the introduced DNA is expressed predominantly by somatic cells (e.g., cardiomyocytes, keratinocytes, and fibroblasts), it is known that relatively small but biologically significant numbers of DCs are transfected with the inoculated DNA (42–44). Based on this fact, the inoculated SOCS1 DNA may have inhibited DC activation through the direct transfection into DCs; however, our data do not exclude the possibility of another indirect mechanisms.

In the EAM model, activation of TLRs on self-Ag–presenting DCs is essential for the expansion of autoreactive $CD4^+$ T cells to induce myocarditis and heart failure (15). We previously reported that *Tlr4* mutant C3H/HeJ mice are resistant to development of EAM (45). Furthermore, IL-1 type 1 receptor signaling on DCs is critical for autoimmune myocarditis development (11). MyD88 is a crucial common adaptor molecule that mediates both TLRs and IL-1 type 1 receptor activation (46, 47), and MyD88 signaling in DCs is critical for the induction of EAM (16). SOCS1 negatively regulates the MyD88-dependent pathway by interacting with both IL-1R–associated kinase and NF-κB (17), which results in a decrease in the induction of inflammatory cytokines such as TNF-α and IL-6. In fact, production of these inflammatory cytokines was inhibited by the administration of SOCS1 DNA in the current study (Fig. 7C). Although nearly all TLRs recruit MyD88, other specific adaptor proteins function downstream of particular TLRs. One such adaptor molecule is Toll/IL-1R domain-containing adaptor protein/Mal. SOCS1 also binds to tyrosine-phosphorylated Mal through its interaction with Bruton's tyrosine kinase, leading to the suppression of Mal-dependent p65 phosphorylation and transactivation of NF-κB (48). Another important mechanism of the suppression of APC activation by SOCS1 is inhibition of the secondary activated JAK–STAT pathway (49, 50). The Toll/IL-1R domain-containing adaptor protein-inducing IFN-β–IFN-regulatory factor 3 pathway rapidly induces IFN-β, which in turn activates JAK–STAT1 and contributes to the expression of IFN-